OTH 94 438

HSE
Health & Safety Executive

WAVE LOADING DATA FROM FIXED VERTICAL CYLINDERS WITH SIMULATED HARD MARINE FOULING

Prepared by Imperial College
for the Health and Safety Executive

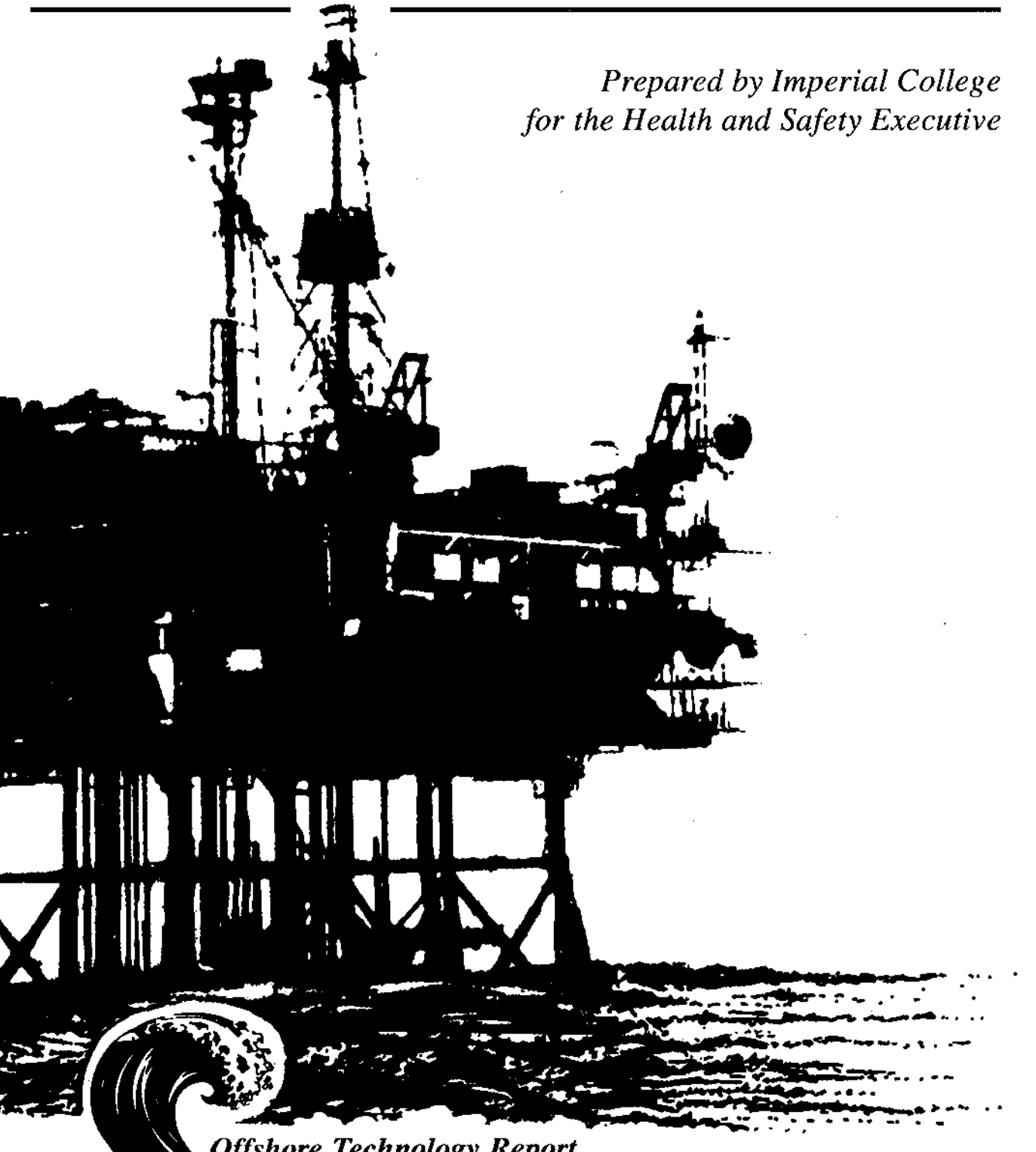

Offshore Technology Report

Health and Safety Executive

OTH 94 438

WAVE LOADING DATA FROM FIXED VERTICAL CYLINDERS WITH SIMULATED HARD MARINE FOULING

Authors

P W Bearman, J M R Graham and P F Hall

Department of Aeronautics
Imperial College
London
SW7 2BY

HSE BOOKS

Health and Safety Executive - Offshore Technology Report

First published 1995
ISBN 0-7176-0999-5

Results, including detailed evaluation and, where relevant, recommendations stemming from their research projects are published in the OTH series of reports.

Background information and data arising from these research projects are published in the OTI series of reports.

SUMMARY

This report describes the analysis of nominally in-line force data measured on roughened, vertical cylinders in random waves. In one experiment a cylinder was tested in random unidirectional waves in a large wave flume (DeVoorst, NL). In another, a cylinder of similar size was exposed to waves in the sea (Christchurch Bay, UK). Both cylinders which had been tested previously under smooth surface conditions were covered in large size pyramidal roughness to simulate hard marine fouling. In the flume tests the cover was total, and in the sea tests only partial coverage was used. A previously developed phase independent data analysis method due to Davies [8] was first used to derive force coefficients from the data. Finally, an improved method was used which computed the phase difference between the velocity and the force to minimise the error between prediction and measurement. Results were also compared with wave by wave force analysis of the cylinder in random and regular waves in the flume for which the relative phase of velocity and force was known.

CONTENTS

LIST OF FIGURES

NOTATION

A	constant incorporating C_d
B	constant incorporating C_m
C_d	drag coefficient
C_f*	total force coefficient
C_{lrms}	rms lift force coefficient
C_m	inertia coefficient
D	cylinder diameter
E^2	mean square error
$F(t)$	measured in-line force on cylinder
F_D	rms drag force
$F_l(t)$	measured transverse force on cylinder
F_M	rms inertia force
$F_x(t)$	force measured in x-direction
$F_y(t)$	force measured in y direction
KC	Keulagan-Carpenter number
K_r	mean roughness height
K*	modified version for KC for non-sinusoidal waves
L	measuring length of cylinder
R_{xy}	cross-correlation of the quantities x and y
$u(t)$	measured velocity
$\dot{u}(t)$	measured acceleration
U_0	amplitude of fundamental component of velocity signal
Δ	time lag
ρ	density of water
$\overline{\Theta}$	mean direction of a quantity
τ	time lag used in correlation functions
$< >$	time averaging of the enclosed quantity

1. INTRODUCTION

Experiments conducted at the Christchurch Bay Tower (CBT) during 1986/87 to measure wave loading on an artificially roughened vertical circular cylinder have been reported by Bishop [7]. The forces were measured on 0.535m long instrumented sections of a 0.48m diameter cylinder. For these tests large pyramidal roughness was distributed over the force sleeves and to a distance of approximately 0.23m either side but not elsewhere. Drag and Inertia force coefficients were computed using the mean square method described by Bishop [7].

The results from similar experiments conducted at the Delta Flume in the Netherlands (DHL) have been described by Wolfram [10]. In this case the force sleeves were 0.25m in length and the same pyramidal roughness was used but with total coverage over the cylinder. Drag and Inertia coefficients were computed from this data by two methods firstly, using cross correlation between the forces and the incident velocity by Fourier averaging and least squares techniques, and secondly, using the Explicit Mean Square method of Davies [8].

Differences in the Drag, Inertia and Total Force coefficients are found between these two sets of data, detailed in [1] although there was generally good agreement between the different methods used to analyse the wave flume data. The wave loading predicted using the coefficients from the laboratory tests is generally higher than that found when the coefficients from the Christchurch Bay Tower are used. However, it should be noted that different analysis techniques were used in the two investigations to extract the coefficients from Morison's equation. The primary aim of the present work is to re analyse the two data sets using a common method to calculate the wave loading coefficients.

2. EXPERIMENTS

2.1 ROUGHNESS DEFINITIONS IN THE DHL AND CBT EXPERIMENTS

The roughness cover used in both experiments was designed and constructed by Wolfram at the University of Strathclyde. The roughness 'shells' were in the form of semi-circular sections which were then clamped to the cylinder. The surface of the shells was made up of a random arrangement of square based pyramids of three different heights 10, 20 and 30mm. The base of each pyramid was equal to its height. The numbers of each size of pyramid varied with there being approximately twice as many of the smallest pyramids as the largest. The bases of the pyramids covered approximately 70% of the total area of each roughness shell. The Department of Energy guidelines[2] state that the effective diameter of a cylinder covered with marine growth is equal to the cylinder diameter plus twice the mean marine growth thickness, Figure 1. The definition of mean marine growth thickness is unclear. Bishop [7] calculates it as the total volume of the roughness divided by the area it covers. A different definition could be the mean height of the roughness assuming a high degree of coverage or simply the Root Mean Square (RMS) value of the surface height. The first definition yields a value of 6mm for the thickness, the second a value of 17.4mm whilst the RMS value is 10.1mm. The fibreglass base of the roughness shells was 3 - 4mm thick, adding 6 - 8mm to the cylinder diameter. Thus it would appear that the diameter of each cylinder should be increased by 19mm according to the first definition of growth thickness, 41.8mm according to the second and 27.2mm for the third. The definition of the cylinder diameter is important as it can have a pronounced effect on the determination of wave loading coefficients and hence the prediction of the forces. The variation in diameter from the above calculations is approximately 4.5% of the nominal cylinder diameter. This would lead to a change in calculated drag coefficient, C_d, of the same percentage, whilst the inertia coefficient, C_m, could change by approximately 9%. This is obviously a matter of significance.

2.2 CHRISTCHURCH BAY TOWER (CBT) TESTS

The experimental set-up at the CBT has been described in detail in a number of references, most appropriately [1] and [7]. A 480mm diameter cylinder was used with the artificial roughness shells described above attached to the force measuring sleeves. The length of the sleeves was 535mm. The diameter quoted in [7] is 508mm, an increase of 28mm on the basic diameter of the cylinder. This has been calculated by using the volume of the pyramids to calculate the mean surface roughness. The extra diameter of 28mm is rather larger than that calculated above (19mm) and although it is not known how exactly the roughness shells were attached to the cylinder, it is assumed they were mounted in the same manner as those at the Delta Flume. The relative roughness height, K_r/D, is however based on the mean height of the pyramids and is quoted as 0.039. Due to the fact that the roughness shells only covered the force sleeves plus a small length, approximately 232mm, either side of each sleeve, the total roughness cover at CBT was 55% of the submerged length of the cylinder. The velocities were measured using perforated ball instruments attached on arms projecting from the test cylinder at each force measuring station. The arms extended approximately 1600mm from the centre of the test cylinder perpendicular to the mean wave direction. The general layout is shown in Figures 2 and 3

2.3 DELTA FLUME (DHL) TESTS

A cylinder with a base diameter of 500mm was used at the Delta Flume during Sep/Oct 1986. During this period a number of tests were carried out with different roughness conditions. Large scale roughness, with pyramids of the same height and arrangement as used at the CBT, was attached to the cylinder for part of the tests. According to [10], the reference

diameter of the cylinder was 521mm, with a mean roughness height of 4% of the diameter. It would appear from the calculations presented in 2.1 that the diameter is again based on the volume of the pyramids whilst K_r/D is calculated using the mean roughness height. The cylinder was completely covered with roughness along its entire length. The measuring sleeves were 250mm long and located 1.5m and 2.5m below mean water level as shown in Figure 4. Velocities were measured by electro-magnetic gauges positioned at the same level as the force sleeves approximately 2m to one side of the cylinder perpendicular to the wave direction. Both regular wave and random wave tests were carried out.

3. ANALYSIS METHOD

Morison's Equation for the in-line force per unit length of a circular cylinder can be written as

$$F(t) = Au(t)|u(t)| + B\dot{u}(t) \qquad (1)$$

where $A = \frac{1}{2}\rho C_d D$ and $B = \frac{1}{4}\pi\rho C_m D^2$

When waves are regular and uni-directional, values for A and B may be found by 'Fourier Averaging' or by the least squares fitting method. In the first method equation (1) is successively multiplied by u(t) and $\dot{u}(t)$ and integrated over a period T. This results in two further equations

$$\langle F(t)u(t)\rangle = A\langle |u^3(t)|\rangle + B\langle u(t)\dot{u}(t)\rangle \qquad (2a)$$

$$\langle F(t)\dot{u}(t)\rangle = A\langle u(t)|u(t)|\dot{u}(t)\rangle + B\langle \dot{u}^2(t)\rangle \qquad (2b)$$

These simultaneous equations can be solved to yield values of A and B. In regular wave data, the integration is normally performed over the wave period T, or a multiple thereof, resulting in the product $\langle u(t)\dot{u}(t)\rangle$ and hence $\langle u(t)|u(t)|\dot{u}(t)\rangle$ being zero. In the least squares method, the mean square error between the measured and reconstructed forces is minimised, and the following is obtained

$$\langle F(t)u(t)|u(t)|\rangle = A\langle u^4(t)\rangle + B\langle u(t)|u(t)|\dot{u}(t)\rangle \qquad (3a)$$

$$\langle F(t)\dot{u}(t)\rangle = A\langle u(t)|u(t)|\dot{u}(t)\rangle + B\langle \dot{u}^2(t)\rangle \qquad (3b)$$

Again, the integration is usually performed over a wave period such that:

$$\langle u(t)\dot{u}(t)\rangle = \langle u(t)|u(t)|\dot{u}(t)\rangle = 0$$

Using these equations, the value for B and hence C_m is identical to that found by solving equations (2). The values of A and hence C_d are different for each method but usually not significantly so. Although these methods are generally used for analysing regular waves, there is no reason why they cannot be used for the analysis of unidirectional random waves also.

In a wave flume, the period and height of the waves can be well controlled and even a set of 'random' waves can be repeated as often as required. Measurements can be made at the most appropriate positions and if malfunctions occur, they can generally be corrected fairly quickly. The same is not true of measurements taken in the sea. Here the waves are random, not necessarily long-crested and may be multi-directional. The directionality especially makes analysis of wave loading data more complex as the definition of the in-line and transverse force directions are unclear. Indeed, the two components of what is normally referred to as in-line force, drag due to velocity and inertia due to acceleration, may not even be in the same instantaneous direction. The second main problem is the measurement of the fluid kinematics.

By necessity, the velocities and accelerations of the fluid cannot be measured at the position of the cylinder and measuring devices must be placed a certain distance away. Even if this distance is substantially smaller than the dominant wavelengths of the waves, there is likely to be a phase difference between the velocity signals and the force signals. The solution of Morison's Equation, using equations (2) or (3), requires that the phase difference between the force and velocity signals is known. Thus not correcting for any phase difference will result in incorrect values of C_d and C_m. Hence in the case of sea data it is obvious that either a phase insensitive method must be used to evaluate the coefficients or the phase must be estimated accurately to facilitate the use of equations (2) and (3). During the period that this analysis was underway an attempt was made to develop a phase independent method. This was initially based on an extension of the Explicit Mean Square phase independent method documented in Davies[8].

This method was an attempt to produce a phase independent solution to Morison's Equation which could be used not only to determine drag and inertia coefficients from sea data, such as that at the CBT, but also to analyse regular, periodic laboratory data such as that obtained in a U-tube. In other words, to provide a single method which could be used to calculate C_d and C_m for all available experimental data, thus eliminating the differences due to data processing which currently exist.

The method made use of the Mean Square equation:

$$\langle F^2 \rangle = A^2 \langle u^2 \rangle + B^2 \langle \dot{u}^2 \rangle \qquad (4)$$

and a second equation generated from the auto-correlation function of Morison's Equation:

$$\langle FF_\tau \rangle = A^2 \langle u|u|u_\tau|u_\tau| \rangle + B^2 \langle \dot{u}\dot{u}_\tau \rangle + AB(\langle u|u|\dot{u}_\tau \rangle + \langle u_\tau|u|_\tau \dot{u} \rangle) \qquad (5)$$

where u and F represent the velocity and force measured at time t, and the subscript τ denoting the same quantities at a time $(t+\tau)$. Thus the quantity $\langle FF_\tau \rangle$ is the auto-correlation function of F(t) at a time lag τ. By selecting an appropriate value of τ, two simultaneous equations (4) and (5) could be obtained to yield values for A and B and hence C_d and C_m. Earlier work had suggested the value of correlating the force with both velocity and acceleration separately. An attempt was therefore made to introduce an auto-correlation with an approximate phase shift of $\pi/2$. Davies therefore chose the quantity τ to be equal to one quarter of the wave period, T, or in the case of random waves, one quarter of the average wave period. This method was used, apparently quite successfully, to compare the CBT and DHL smooth cylinder results for random waves, and is documented in the first report on this work (Davies[8]). However, it was found that for a sinusoidal input to u(t), such as that obtained in a U-tube, the equations (4) and (5) were theoretically indeterminate when the value of τ was set equal to T/4 or a multiple thereof, all three terms on the right hand side of (5) becoming identically equal to zero. The results obtained therefore depended upon the random fluctuations in the measured signals and departures from the Morison model. This was not detected in Davies's work as the signals he was examining were predominately random and this randomness generally resulted in a solution. The method was a significant improvement on the use of the Mean Square Equation alone (Bishop[7]) but was not as widely applicable, nor as accurate as had been hoped.

An attempt was made to rectify this problem by extending the method as follows. It is possible to solve the two equations if the value of τ is set to any value except multiples of T/4. In this case, whilst the term involving AB is zero for all values of t, the terms involving A^2 and B^2

vary in a non-linear manner resulting in a pair of determinate equations. The precise selection of value of τ was identified as being of considerable importance. Obviously certain ranges of values would result in two equations which were practically identical and thus poorly conditioned, whilst others would produce the problem described above. It would seem logical that selecting $\tau = T/8$ would be close to the optimum value and indeed from analysing the eigenvalue behaviour of the pair of equations this turns out to be the case.

The method was therefore modified in this way and tested on real data. Initially regular wave data was used as it is possible to verify the results using alternative methods such as the least squares method. The results were not initially encouraging as the resulting data tended to be somewhat scattered. An in-depth examination of the effect of the value of τ was then undertaken and although a method was devised where the optimum value was chosen for each wave, it was still found that the results were highly dependent on the precise value chosen. It is difficult to ascertain the exact reason for this but again the fact that the signals contain some degree of noise and also the influence of departures of the actual force from the Morison form may account for the difficulty in solution.

A further development was therefore introduced utilising all possible auto-correlations of the data, i.e. all possible values of τ. Equation (4) is a result of (5) with τ being set to zero. It was thought that if the auto-correlation function was computed for all values of τ, then the least-squares method could be used to find a solution to A and B which would not depend on any phase difference between the force and velocity signals. Denoting the cross-correlation of two quantities x and y as R_{xy}, where

$$R_{xy} = \langle (x(t)y(t+\tau)) \rangle \tag{6}$$

equation (5) can be re-written

$$R_{FF} = A^2 R_{u|u|u|u|} + B^2 R_{\dot{u}\dot{u}} + AB\,(R_{u|u|\dot{u}} + R_{\dot{u}u|u|}) \tag{7}$$

Applying the usual least squares method to this equation results in the following two simultaneous equations from which A and B can be solved

$$\left[A^2 R_{u|u|u|u|} + B^2 R_{\dot{u}\dot{u}} + AB(R_{u|u|\dot{u}} + R_{\dot{u}u|u|}) - R_{FF}\right] \times \left[2A R_{u|u|u|u|} + B(R_{u|u|\dot{u}} + R_{\dot{u}u|u|})\right] = 0 \tag{8a}$$

$$\left[A^2 R_{u|u|u|u|} + B^2 R_{\dot{u}\dot{u}} + AB(R_{u|u|\dot{u}} + R_{\dot{u}u|u|}) - R_{FF}\right] \times \left[2B R_{\dot{u}\dot{u}} + A(R_{u|u|\dot{u}} + R_{\dot{u}u|u|})\right] = 0 \tag{8b}$$

Whilst it is theoretically possible to solve these two equations and a 'perfect' test signal demonstrated the feasibility of the method, it is necessary to calculate high moments of the measured quantities, u^8, $\dot{u}^4$ and F^4. The numerical errors involved in calculating these quantities were found to dominate the solution of the equations and although considerable effort was expended on this problem, the method was deemed to be unsatisfactory.

Whilst not identical, an analogy to methods based on the above approach is to solve both the Mean Square equation (4) in conjunction with the Kurtosis function

$$\langle F^4 \rangle = A^4 \langle u^8 \rangle + B^4 \langle \dot{u}^4 \rangle \tag{9}$$

A graphical representation of the solution of the simultaneous solution of equations (4) and (9) is shown in Figure 5. It can be seen that the intersection points on the two curves, which represent both a correct and an incorrect solution for A and B, are not well defined and in practice only a small deviation from the theoretical solution is required to make large changes to the position of the correct intersection point and hence the values of A and B.

In view of the failure to find a satisfactory solution to these phase independent methods, a development was designed which estimates the phase. The technique is based on the least-squares method using equation (3). The mean square error between the measured force and the reconstructed force is equal to

$$<E^2> = <(F(t) - (Au(t)|u(t)| + B\dot{u}(t)))^2> \qquad (10)$$

Differentiating this equation with respect to the two unknowns, A and B, results in equations (3a) and (3b). In a random sea, the various wave components will travel with their own velocity. Ignoring the directionality problem for the moment, it is obvious that a velocity measuring device placed either upstream or downstream of the measuring cylinder will not reflect exactly the kinematics of the fluid at the cylinder itself, even allowing for a mean time delay for the waves to travel from the probe to the cylinder. In theory, it should be possible to decompose the velocity signal into a number of components and using wave theory, reconstruct the correct velocity signal which would be measured at the cylinder itself. Unfortunately wave theory is not at a stage where this can be done simply or reliably. In practice, if the velocity probe is only a short distance from the cylinder, it is reasonable to assume that the velocity recorded by the velocity probe will be incident upon the cylinder a short period later. At the CBT the probes were approximately 1.6m from the cylinder. Even if the waves were approaching the cylinder perpendicular to a line connecting the velocity probe and the cylinder, a 10sec wave, with a wavelength of 90m, the dominant period throughout the tests examined here, would take only 0.18secs to travel from the probe to the cylinder. In practice, since the waves at CBT generally travel normal to a plane containing the cylinder and the wave probe, as shown in Figure 3, this time difference is likely to be considerably less. However knowing how sensitive the solution of Morison's Equation is to the relative phase between the force and the velocity, it is important to attempt to estimate the phase error by calculating the time difference as precisely as possible.

It can thus be seen that the equation which has to be solved, (1), now becomes

$$F(t+\Delta) = Au(t)|u(t)| + B\dot{u}(t) \qquad (11)$$

where Δ is the time difference between the force and velocity signals and is unknown. Substituting this into equation (10) results in

$$<E^2> = <(F(t+\Delta) - (Au(t)|u(t)| + B\dot{u}(t)))^2> \qquad (12)$$

In theory, differentiating this with respect to the three unknowns A, B and Δ, would result in three simultaneous equations, the solution of which would minimise the mean square error $<E^2>$. Unfortunately this is a somewhat difficult procedure as the differentiation with respect to Δ of equation (6) results in an intractable integral equation which is impossible to solve directly. The method of solution which has been adopted here is that for a given value of Δ,

the mean square error is minimised as normal and the coefficients A and B found using (3). The mean square error is then calculated using (12). This procedure is then repeated for a number of values of Δ and the value of Δ which produces the minimum mean square error is assumed to be the correct one. Figure 6 shows how the mean square error varies for a sine wave input to u(t). A test signal of this form was used to check the results of the computer program.

The method was also tested on data from the Delta Flume where the phase difference between the velocity and force signals was zero. The value of Δ found should thus have also been equal to zero. As might be expected with large scale laboratory data, the values of Δ were not always equal to zero but the program returned values which were normally less than 0.1sec corresponding to 5 sample intervals. It was also noted that the effect the variation had on the values of C_d and C_m was slight. The results were generally changed by less than 10% which was thought to be within acceptable limits given the difficulty in examining data of this nature and the problems discussed in this section.

4. RESULTS

In this report the CBT data which was taken in random seas and both the DHL random and regular wave data were analysed. In each case the cylinder surface condition was that of the large roughness simulating hard marine fouling. To be consistent with Bishop's analysis, the definition of Keulegan-Carpenter number used was

$$K^* = \frac{4\pi}{D}\left\{\frac{<u^4>}{3<\dot{u}^2>}\right\}^{1/2} \tag{13}$$

For single component regular waves this reduces to the usual definition

$$K^* = KC = U_0T/D \tag{14}$$

Drag and Inertia coefficients are defined as in (1) and a total force coefficient C_f^* defined, after Bishop[6], as

$$C_f^* = \left[\frac{<F^2>}{(\tfrac{1}{2}\rho DL)^2 \left(<u^4> + \left(\frac{\pi D}{2}\right)^2 <\dot{u}^2>\right)}\right]^{1/2} \tag{15}$$

This can also be written as

$$C_f^* = \left[\frac{C_d^2 \frac{3K^{*2}}{4} + C_m^2}{\frac{4\pi}{\frac{3K^{*2}}{4\pi} + 1}}\right]^{1/2} \tag{16}$$

assuming the measured force is adequately characterised by the Morison model. It can thus be seen that as K* approaches zero, C_f^* approaches the value of C_m and as K* increases C_f^* approaches C_d.
The RMS lift coefficient is defined as

$$C_{lrms} = \frac{<F_l^2>}{\tfrac{1}{2}\rho DL<u^2>} \tag{17}$$

The question of the appropriate cylinder to be used has been discussed in section 2.1. To enable comparison with the existing data from previous reports the measurements stated by the different researchers have been used, i.e. 508mm for the CBT data and 521mm for the cylinder at the Delta Flume. However the discrepancy between the two diameters should be noted. Given that the roughness shells were identical, allowing for the difference in the base diameters of the cylinder, and the methods of calculating the effective diameter appear to be the same, it is surprising that the increase in diameter is significantly different for each cylinder, 21mm for the Delta Flume experiment and 28mm for that at CBT. This results in an uncertainty in C_d of 1.4% between the two sets of results with a difference of 2.8% in C_m, with the expectation that the results at CBT should be lower by these amounts. The density of sea water has been assumed to be 1030 kg/m^3.

4.1 DELTA FLUME REGULAR WAVES

The Delta Flume coefficients for regular waves are shown in Figures 7, 8, 9 and 10. The coefficients are obtained by analysing each record on a wave by wave basis and finding the drag and inertia coefficients by the least-squares method. The mean values of K*, C_d, C_m and C_f* were then computed for each run. It can be seen from Figure 7 that there is little difference in C_f* between the upper and lower force sleeves and a general decrease in C_f* with K*. Examination of Figures 8 and 9 show that there is some scatter in C_d and C_m, especially for the inertia coefficient at K* values between 8 and 15. Over the same range of K*, high values of C_{lrms}, Figure 10, are recorded. Careful inspection of individual wave records show that C_d and C_m may vary considerably during a run and indeed waves at the beginning of the run may produce considerable different values from those at the end. This effect is demonstrated in Figure 11. This is also accompanied with slight changes in K* during a run as the effect of reflections from the beach at the flume influence the wave maker control system. It should be emphasised that these changes in conditions are slight yet can have a pronounced effect on the force coefficients, although the actual forces on the cylinder may not change significantly, as reflected in the consistency of C_f*.

At low K*, it is noted that the potential flow value of C_m = 2 is exceeded and that the values of C_d are scattered. The second effect is principally due to the fact that the drag contributes little to the total force and C_d is thus difficult to obtain with any degree of accuracy. Figure 12 shows the variation of the ratio of RMS drag force to RMS inertia force using the coefficients from this set of data. It can be seen that below K* of 10, inertia dominates and above 10 drag very quickly becomes the major force. Why values of C_m greater than 2 are obtained is unclear. Due to the difficulties in calculating a precise cylinder diameter, the increase in C_m of approximately 5% to a value of 2.1, could be accounted for by increasing the cylinder diameter by 2.5%, to 534mm. This diameter would still be consistent with the various definitions of roughness given in section 2.1.

4.2 DELTA FLUME RANDOM WAVES

In addition to the regular wave tests carried out at the Delta Flume, 3 hours of random wave testing was also performed. The wave spectrum was of the JONSWOP form with a peak period of 5.9secs and a significant wave height of 1.5m. Analysis was carried out by using the method described with a minimum integration period of 23.6 secs. The integration period was extended beyond this so as to examine a period containing a number of complete waves. This ensured that the product $< u(t)\dot{u}(t) >$ was as close to zero as possible, although its actual value was taken into account in the computations. The results exhibited considerable scatter as shown in Figures 13, 14, 15 and 16, although the consistency in C_f* is quite remarkable. For this reason the results have been averaged over small bands of K* to produce mean coefficients. Every value plotted in Figures 17, 18, 19 and 20 is an average of a group of results over a band of K* = 0.5. It can be seen from Figure 17 that there is a slight difference

in C_f*, of approximately 7%, between the two measuring stations at low values of K*. The difference appears to reduce slightly as K* increases. A similar difference can be seen in C_m, but fairly constant with respect to K*, as shown in Figure 19. However, the drag coefficient, shown in Figure 18, does not exhibit the same systematic difference. There is some variation between values of C_d at similar K* for the two depth stations, increasingly so at low K*, but not always of the same sign. The variation of C_d and C_m with K* over the range K*=8-15 that was apparent in the regular wave tests (figures 8 and 9), is not manifested in the results from random wave testing (figures 18 and 19). A clearly defined rise in C_{krms} over the same range of K* is similarly not evidenced in the case of the random wave data (figures 10 and 20)

4.3 CHRISTCHURCH BAY TOWER

The additional problem in computing coefficients for the CBT was the fact that the waves are multi-directional. Initially it was decided to calculate the mean force direction from the equation

$$\tan 2\overline{\Theta} = \left[\frac{2 < F_x F_y >}{< F_x^2 > - < F_y^2 >} \right] \qquad (18)$$

where the x-axis is defined in Figure 3 and $\overline{\Theta}$ is the mean force direction relative to the x-axis. This was done both with and without the mean force components removed. The angle $\overline{\Theta}$ was found to vary between 3° and 16°. The mean velocity and acceleration directions were also found in the same way. The mean velocity vector was found to vary between -13° and 4° and the acceleration direction from between 0° and -10°. There being no consistency between the force and fluid directions and the angles themselves being fairly small, it was decided to accept the x-direction as being the mean in-line force direction. Figure 21 shows typical error function results for three waves, calculated using equation (10). It can be seen that the minimum mean square error is minimised near a point representing zero phase difference between the velocity and force signals. This would appear to confirm that the mean wave direction was close to the x-axis.

The data was then analysed in the same way as that for the Delta Flume except that the period of integration was increased to 40secs to account for the fact that the mean period of the waves, obtained from spectral analysis of the velocity records, was approximately 10secs. Five complete sets of data were analysed, record nos. 14, 15, 19, 28 and 39, see ref.[9]. During the period of recording, the rms wave height varied from between 1.0 and 2.0m. Data was obtained at measuring stations 3, 4 and 5 shown in Figure 2. The results from record 14 are plotted in Figures 22, 23 and 24. Examination of these results shows a similar feature to those in the Delta Flume in so much as the coefficients are generally less at the top station, 3, than at the lower two, 4 and 5. However, the difference is greater, around 10 - 15% and affects all three coefficients. Records 15, 19 and 28 exhibit the same characteristics and cover approximately the same width in K*. Record 39, the results for which are shown in Figures 25, 26 and 27, covers a lower range of K* but exhibits the same variation in coefficients. There appears to be no explanation at present for this variation in coefficients between stations.

The results for all records are summarised in Figures 28, 29, 30 and 31. The data has been averaged in the same manner as for the Delta Flume results. Whilst similar trends are present at all three measuring stations, it is quite clear that the coefficients for stations 3 are significantly different to those for stations 4 and 5. The rms lift coefficient is shown in Figure 31 and surprisingly this appears to show no significant variation with depth.

5. COMPARISON OF RESULTS

5.1 COMPARISON BETWEEN ANALYSED DATA SETS

The results from the Delta Flume and the CBT cover different ranges of K*, with only a small area of overlap. Figure 32 shows all the C_f* results, DHL (random), DHL (regular), and CBT (random) obtained from the present analysis. It can clearly be seen that the two sets of DHL results are quite consistent, the regular and random wave data lying along similar curves. The area of overlap with the CBT data is in the K* range 10 - 15 which, as already discussed, is the range where the greatest degree of scatter can be expected. However, it would appear that within this range the results from CBT stations 4 and 5 are approximately 12% lower than those obtained from the Delta Flume, the results from station 3 showing an even greater discrepancy.

The drag and inertia results are summarised in Figures 33 and 34, respectively. The difference in C_d between the CBT results and the random tests from the Delta Flume can be seen to be fairly slight, although in the region of overlap they are somewhat scattered. It is also obvious that the results from regular wave tests at the Delta Flume and the random tests are significantly different, due to the peak in the drag coefficient at a K* of 10, even though the total force coefficient, C_f*, is very similar.

The inertia coefficient however, shows different characteristics, being significantly higher for the random Delta Flume results than both the regular wave tests and the CBT data over the K* range 10 - 15. This is not entirely suprising since the total force coefficient, C_f*, is higher for the Delta Flume tests than the CBT results and since C_d was the same for both sets of data, it would be expected that C_m would be larger. The regular wave results show an even larger drop in C_m which compensates for the higher drag coefficients found.

The lift results, shown in Figure 35, are too scattered to make a good comparison, although it can be seen that the regular wave results are significantly different from both sets of random data. It is possible that a peak in C_{lrms} occurs in the random data between K* values of 8 and 15 but due to the lack of overlap between the two data sets, it is difficult to be certain.

Figure 36 shows the ratio of rms drag force to rms inertia force for all three data sets. It can be seen from the random results that although drag is greater above a K* of 15, inertia still makes a significant contribution to the total force. It is also notable that results from the regular wave tests give a false impression of the relative importance of the drag and inertia terms at K* values between 10 and 20.

5.2 COMPARISON WITH PREVIOUS CBT RESULTS

Bishop[7] quotes C_f*, C_d and C_m values for all the 30 records processed in 1987. Figures 37, 38 and 39 show a summary of this data. C_f* was computed over the 20min period of each record, whilst C_d and C_m were obtained by the Mean Square Method detailed by Bishop[5]. It can be seen from Figure 37, that C_f* is generally unaffected by depth, the variations being of the order of 1 - 2%. Comparing this with Figure 28, the results of the analysis performed for this report, the variations of C_f* with K* is greater and at higher values of K*, C_f* is lower than the results obtained here. Values of C_f* obtained from shorter averaging periods in [7] show similar trends. The drag coefficients obtained by the Mean Square Method shown in Figure 38, demonstrate little variation with depth, with station 3 showing the highest values of C_d, the opposite of which is found here. Overall the values are comparable to those found here, if marginally lower. Bishop's "best line fit" for C_m vs K*, shown in Figure 39, shows no variation in C_m with K* although there is a significant change with depth and the values from [7] do show considerable scatter, varying from 1.3 to 2.4 but with no general trend. The

results obtained here, shown in Figure 30, are also scattered but the general trend is for an increase in C_m with K*.

5.3 COMPARISON WITH DELTA FLUME RESULTS

Wolfram, Theophanatos and Bolland [10] analysed the regular wave tests. Their values of C_d and C_m, shown in Figures 40 and 41, show good general agreement with those found here, given that they have plotted their coefficients against KC, based, as far as is known, on the first order component of the velocity signal and the fact noted here that the values are somewhat unstable for certain values of K*. The data has also been analysed by Davies [8] whose values for C_d and C_m also show good agreement with those found here.

The DHL rough cylinder random wave data has been analysed by Davies[8] using the wave by wave method. In general his values of C_m, shown in Figure 43, are similar to those found here, averaging about 2 over a broad range of K*. Davies' results show a marked reduction in C_m at the lowest value of KC, and a small reduction for other values of KC less than 2, which is not reflected in the present results. His values of C_d, Figure 42, are generally higher, remaining above 1.5 for KC less than 15, whereas the values found here in this range of KC are typically 1.2 to 1.3. Both sets of results show an increase in C_d at K* less than 5. Some of the differences between the wave by wave method and the new method are in regions where either the force coefficient is associated with a minor part of the overall force (e.g. C_d at low K*) or where the cylinder is subjected to the smallest waves (all the very low K* data). In the latter case, forces induced by the smallest waves may be strongly affected by the history effect from larger preceding waves in a random wave set. As a result a great degree of scatter is present in the individually computed coefficients prior to averaging and different forms of analysis are more likely to give different results. However, there is a systematic difference in the value of C_d between the results of the two methods over the higher K* range.The new method gives values of C_d about 15% lower than Davies' wave by wave analysis (see figure 18 and figure 48, taken from figure 6.6 in the earlier report [8]). This may be relevant in comparisons with other data where different methods are used. However, differences between the new method and the wave by wave analysis of some specific smooth cylinder data for which it was tested were effectively negligible.

6. CONCLUSIONS

As stated in the introduction, it appeared at the outset of this work that large differences existed between the force coefficients for rough cylinders in tests carried out at DHL and at CBT. This investigation confirms that differences exist between the CBT experiment and the *regular* wave results from the DHL tests. However the differences between the CBT data and the DHL random wave tests are fairly small, the latter returning slightly higher coefficients. This may be explained by the difference in roughness cover in the two tests, the DHL cylinder having full cover but the CBT cylinder only partial cover in the immediate neighbourhood of the force sleeves. There is also an inconsistency in the definition of the mean diameter between the CBT rough surface tests and those undertaken at DHL. In the former tests a larger increment is given to the mean diameter of the basic cylinder for the roughness shells than in the latter tests. A small but inconsistent variation of the coefficients with depth of the measuring station also remains unexplained.

On a final note, it has been seen that large changes in the drag and inertia coefficients are possible, especially in regular waves over a narrow range of K*. This example alone shows the difficulty in obtaining reliable coefficients even when the phase between the force and velocity signals is known precisely. However it should be noted that the variability is not caused simply by some phase variation in the force signal but a departure from the Morison model itself, presumably due to the influence of the transverse or lift force. Figures 44, 45 and 46 show several reconstructions of time histories taken at random from the CBT data analysis of the Morison force, for different specified K* values. It can be clearly seen that the peak force is underestimated, although a systematic analysis of this has not been undertaken. Figure 47 shows a reconstruction of a segment of a data set using both the drag and inertia coefficients taken from the particular data set and from an average of values obtained from runs with that particular value of K*. It can be seen that whilst the coefficients vary by approximately 10%, the peak force predicted is approximately the same in each case, the apparent reduction in inertia loading being compensated by extra drag. If the model itself is not satisfactory, it is perhaps not surprising that the solution exhibits a certain degree of unreliability. It is also noted that the total force coefficient, C_f*, exhibits a high degree of reliability, even when drag and inertia coefficients vary wildly.

REFERENCES

[1] AME Ltd. "*Roughness and Vortex Shedding Effects for Cylinders in Flume and Real Sea Waves*". OTH 91 345, HMSO, 1991

[2] BARLTROP, N. D. P., MITCHELL, G. M. and ATTKINS, J. B. "*Fluid Loading on Fixed Offshore Structures, Volume 1*". OTH 90 322

[3] BEARMAN, P.W. "*Wave loading experiments on circular cylinders at large scale*", Proc. 5th Int. Conf. on the Behaviour of Offshoe Structures, Trondheim, Norway, Tapir, pp 471-487, 1988

[4] BEARMAN, P.W., CHAPLIN, J.R., GRAHAM, J.M.R., KOSTENSE, J.K., HALL, P.F. and KLOPMAN, G. "*The loading on a cylinder in post-critical flow beneath periodic and random waves*", Proc. 4th Int. Conf. on the Behaviour of Offshore Structures, Delft, the Netherlands, Elsevier Science Publishers, pp. 213-225, 1985

[5] BISHOP, J. R. "*The Mean Square Value of Wave Force based on the Morison Equation*". OT - R -7811 (NMI R 40), 1978

[6] BISHOP, J. R. "*A New Coefficient for Total Wave Force*" OT - R - 8017 (NMI R 77), 1980

[7] BISHOP, J. R. "*Wave Force Experiments at the Christchurch Bay Tower with Simulated Hard Marine Fouling*". OTI 89 541, HMSO, 1989

[8] DAVIES, M. J. S. "*Wave Loading Data from fixed Vertical Cylinders*". OTI 92 558, HMSO, 1992

[9] FLUID MECHANICS CONSULTANTS, "*Christchurch Bay Tower Data Catalogue*",1992

[10] WOLFRAM, J., THEOPHANATOS, A, AND BOLLAND, J. "*Marine Fouling and Fluid Loading*", Project FLE6, Marine Technology Directorate

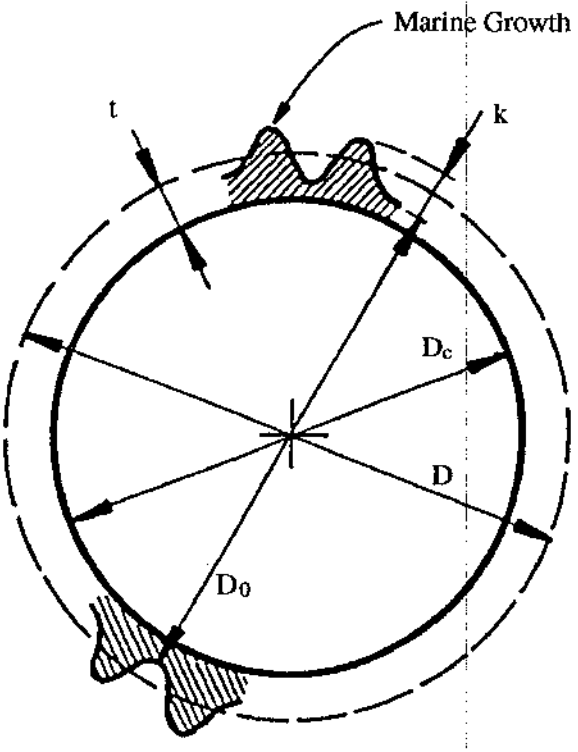

D_c = cylinder diameter

k = mean roughnes height

t = mean marine growth thickness

D = mean diameter of cylinder and marine growth

$D_0 = D_c - k + 2t$

Figure 1 Definition of cylinder diameter

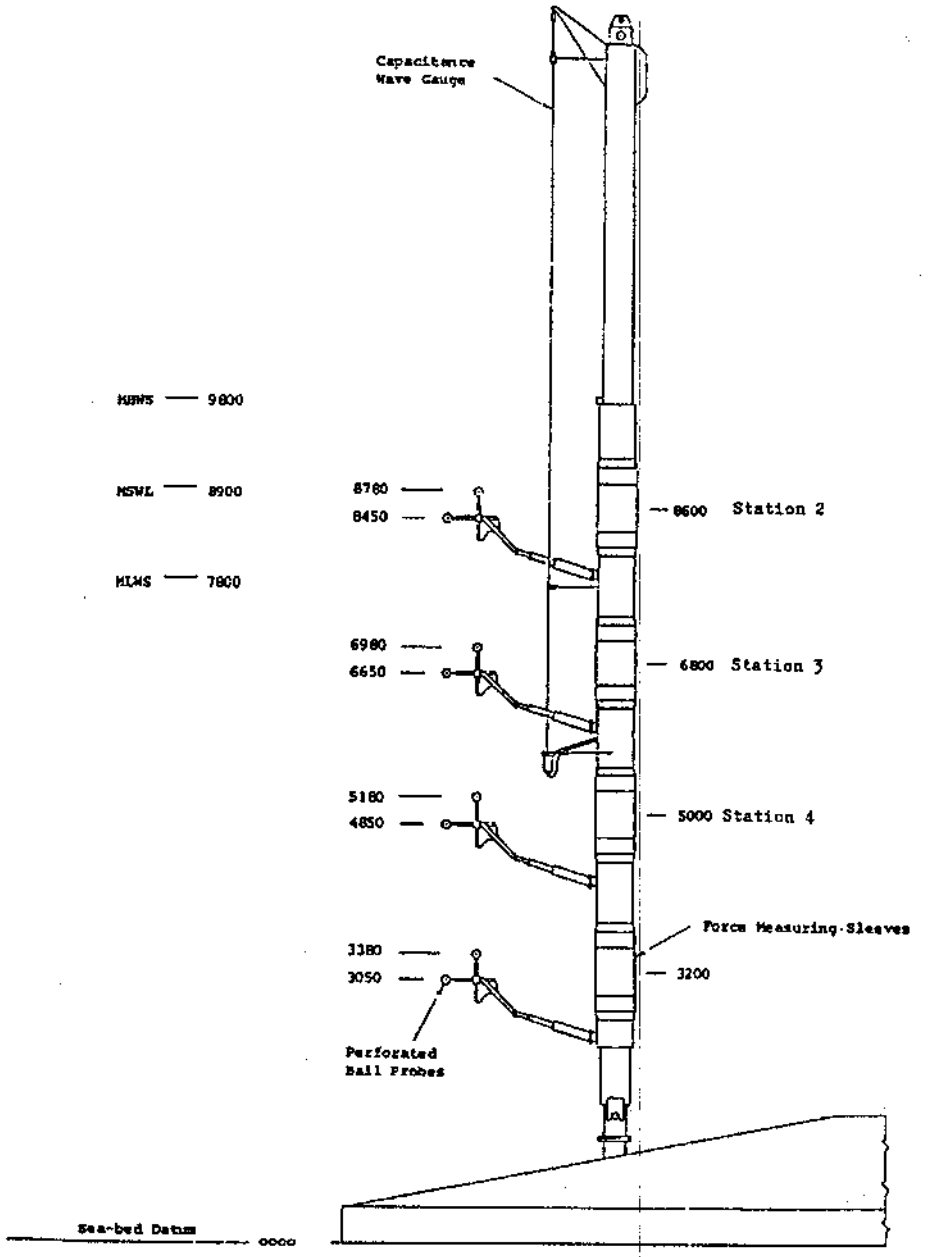

Figure 2 Schematic diagram of small cylinder at CBT showing position of measuring stations

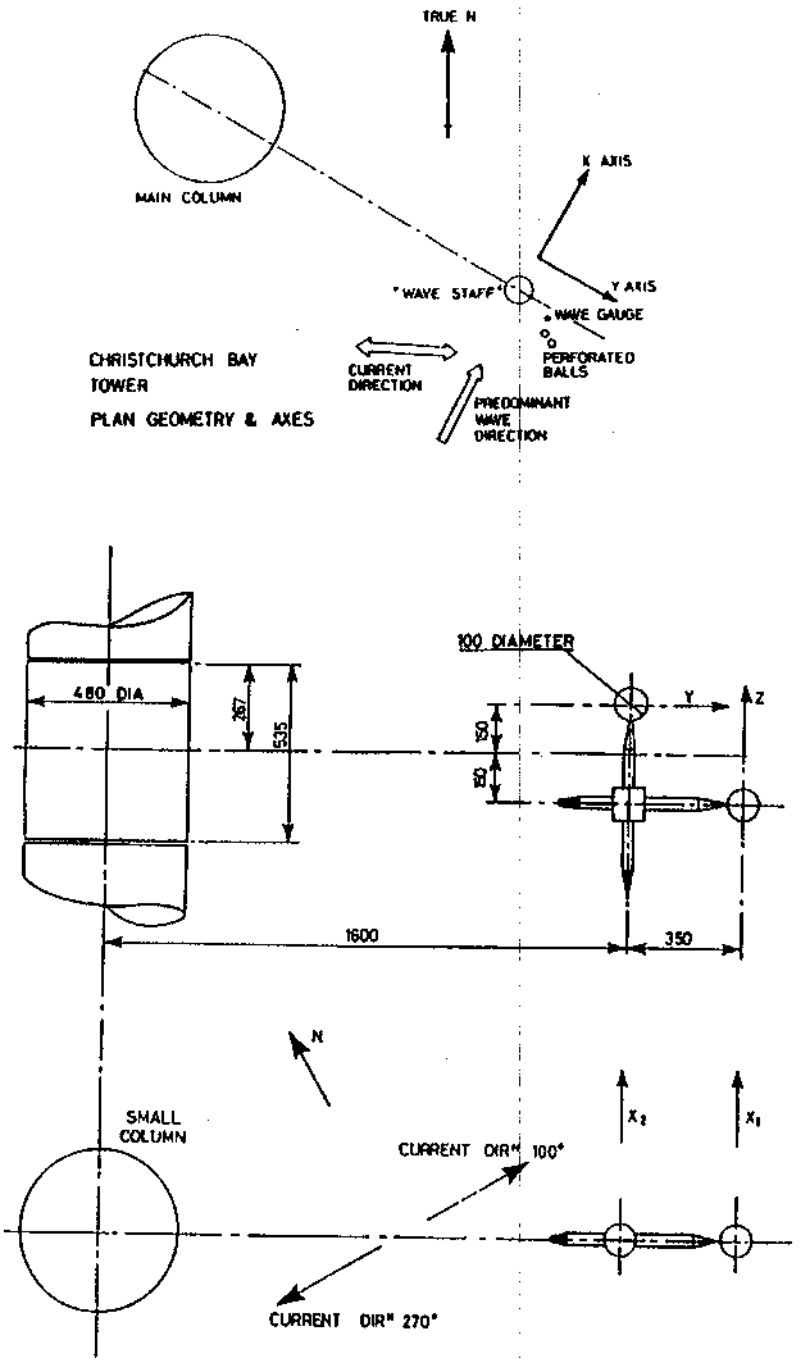

Figure 3 Plan geometry and velocity instrument location at CBT

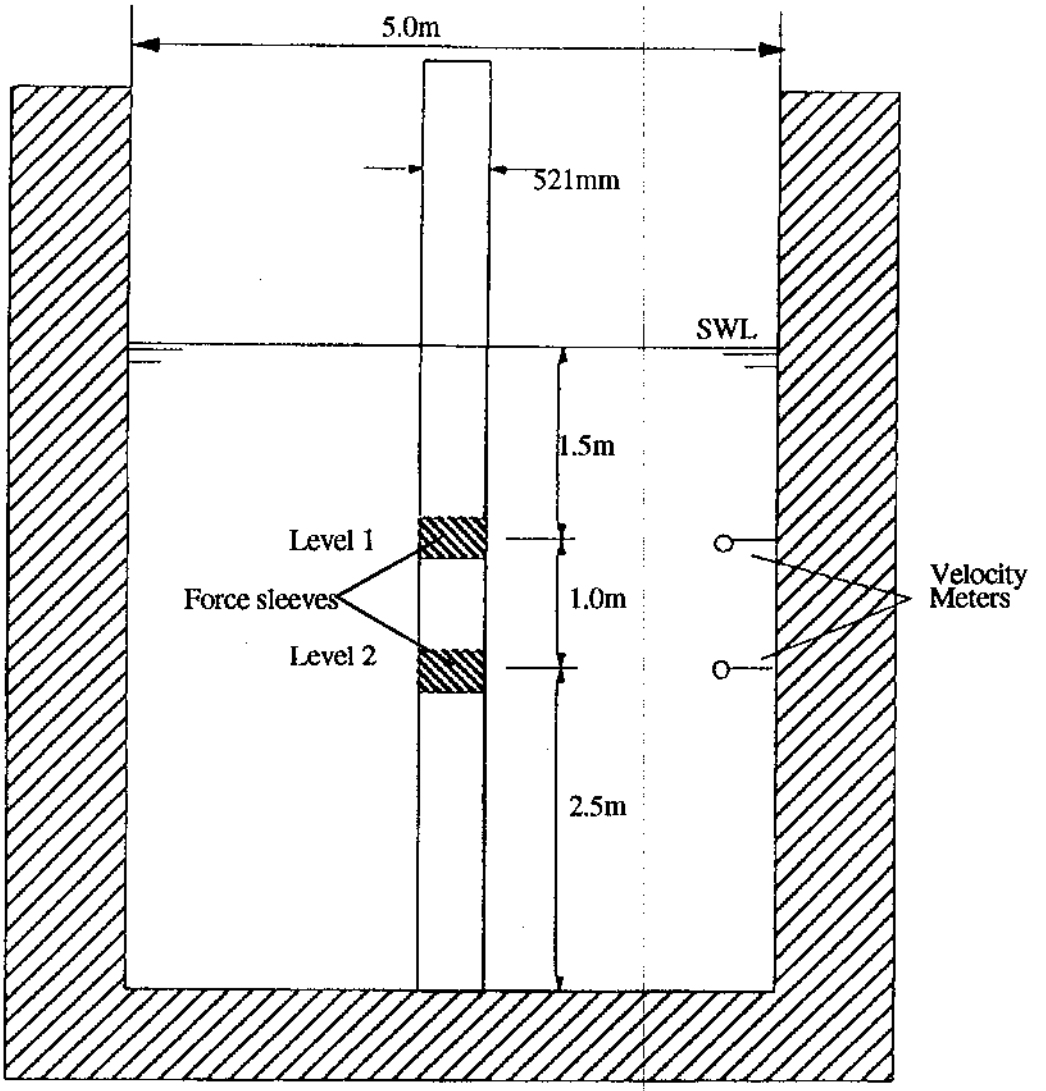

Figure 4 Schematic diagram of cylinder mounted at the Delta Flume

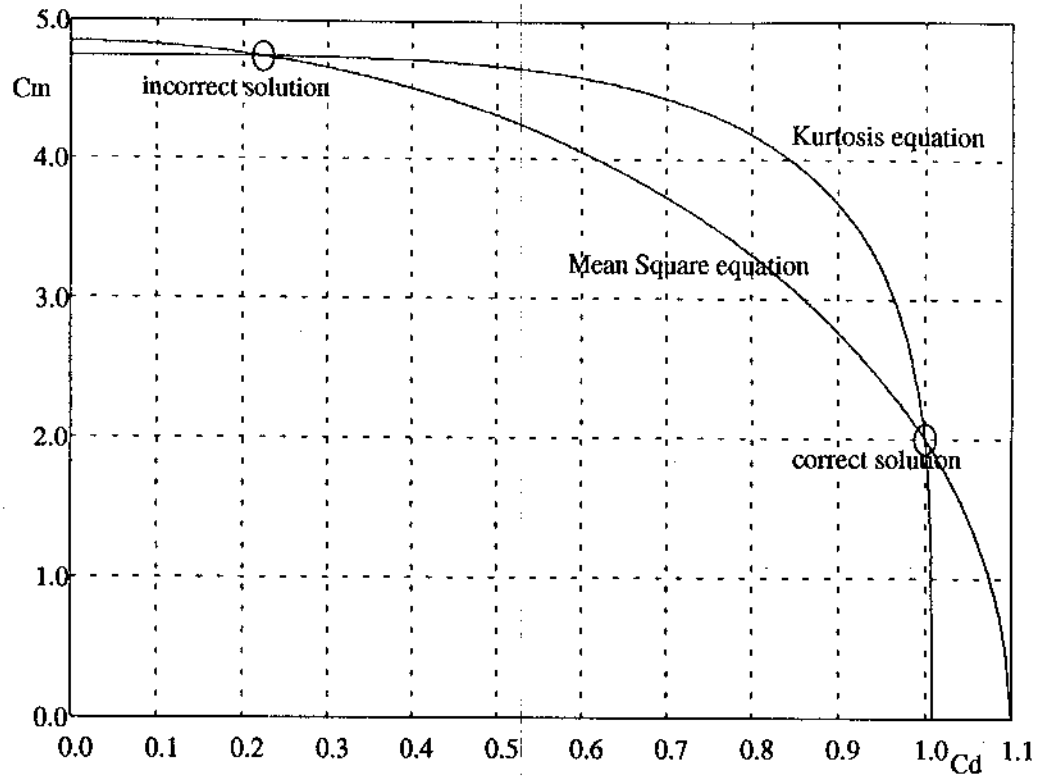

Figure 5 Solution of the Mean Square and Kurtosis equations

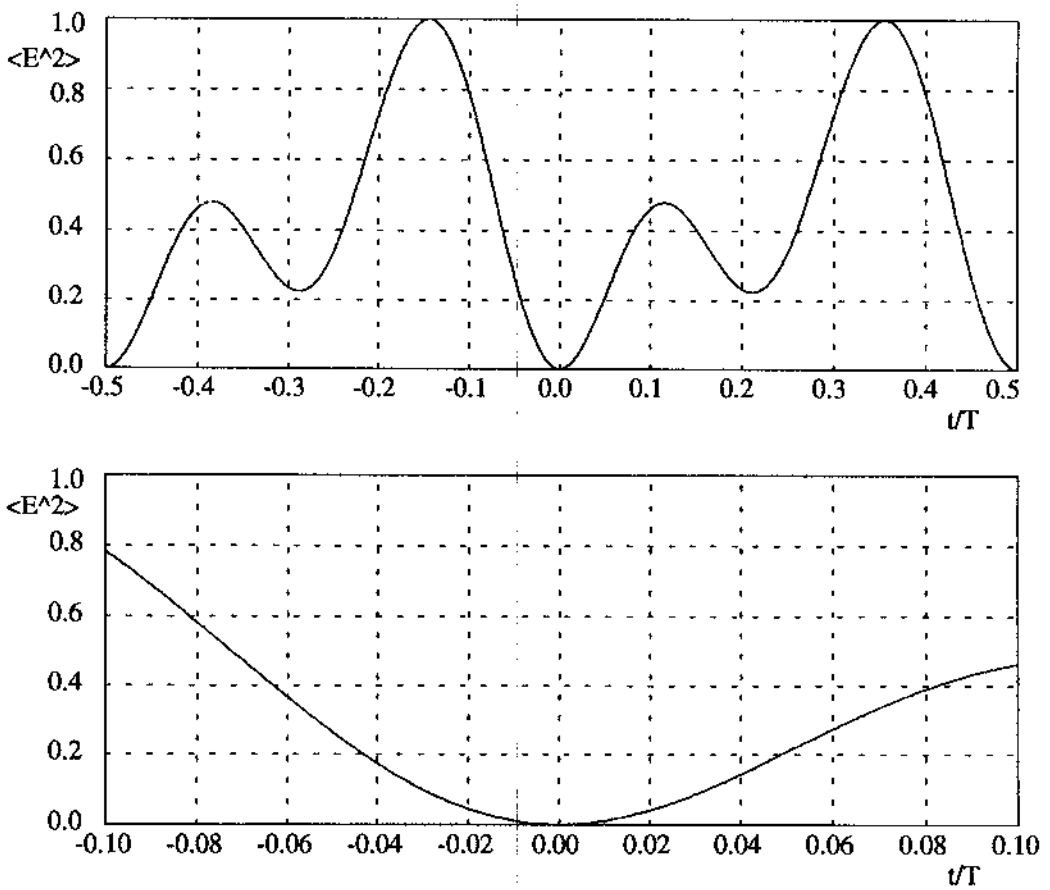

Figure 6 Normalised mean square error for a sine wave input to u(t)

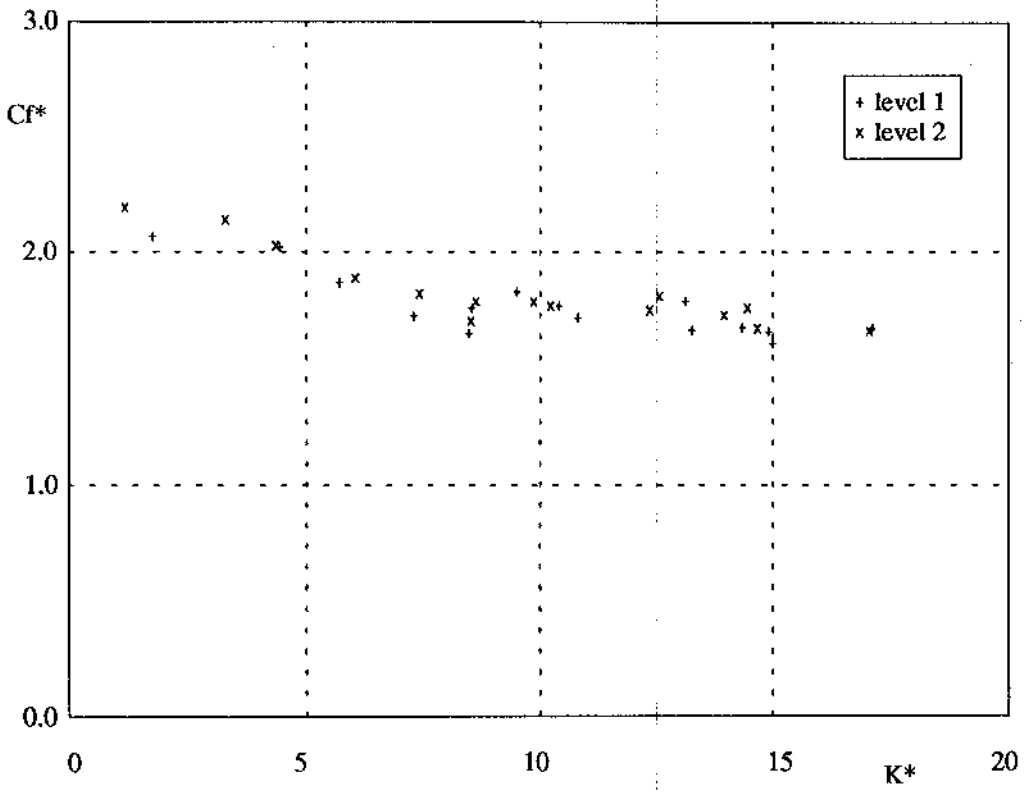

Figure 7 Cf* v's K* - regular waves at the Delta Flume

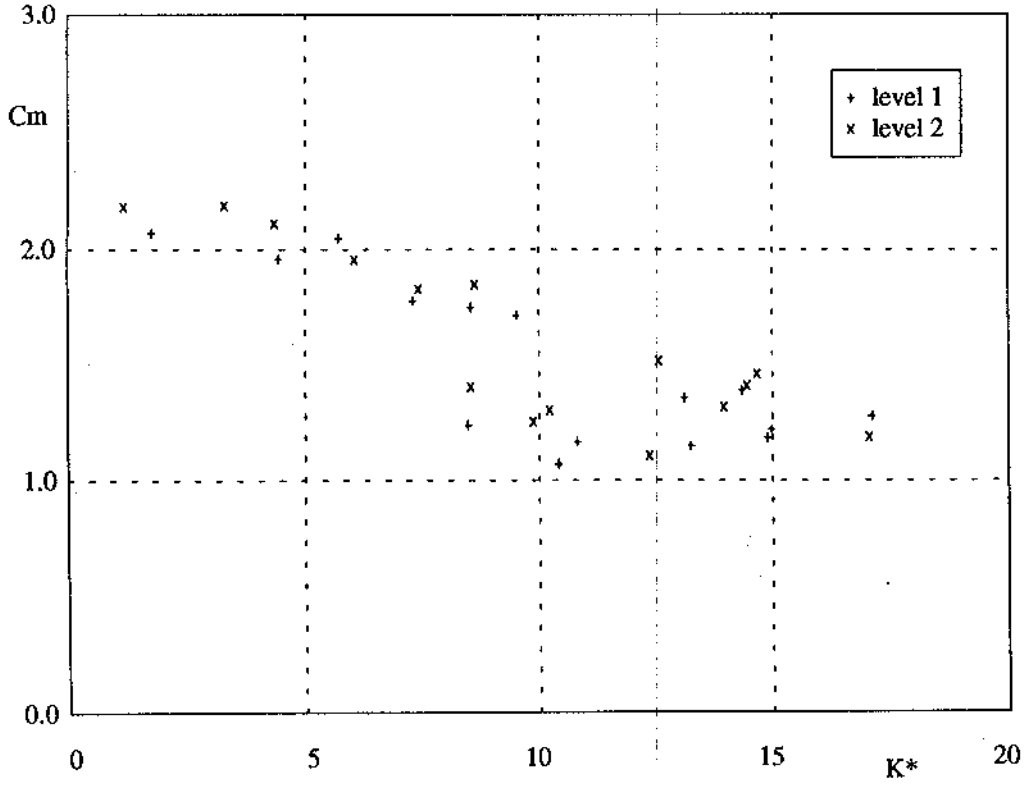

Figure 8 Cm v's K* - regular waves at the Delta Flume

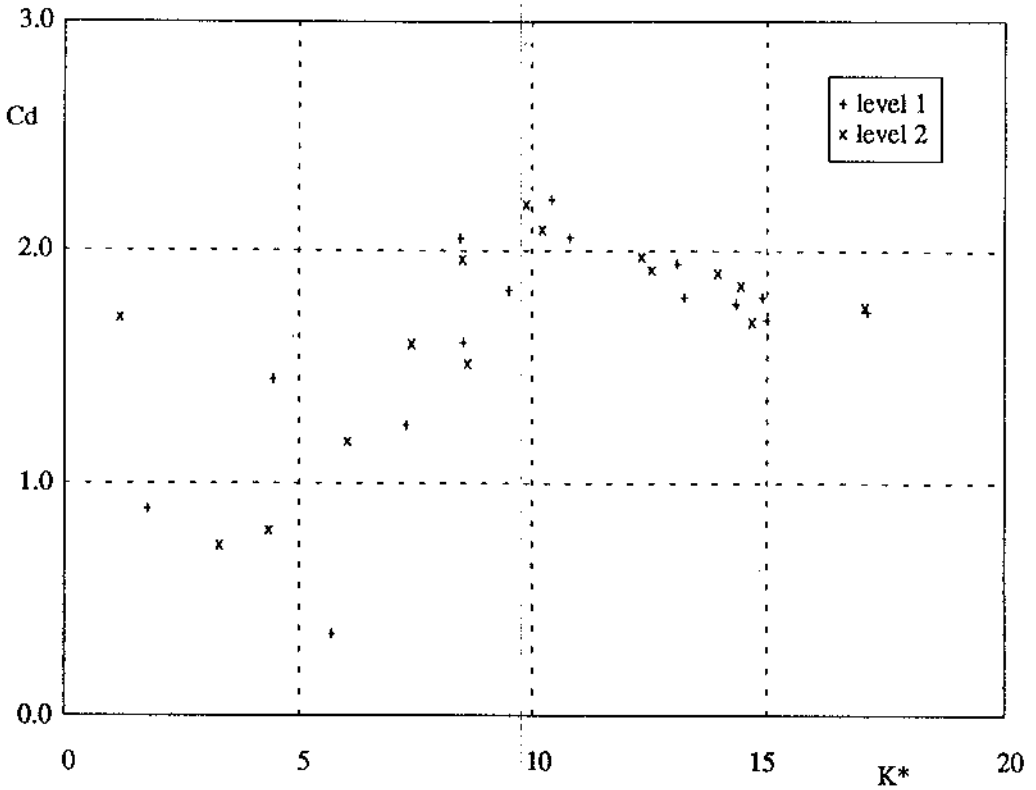

Figure 9 Cd v's K* - regular waves at the Delta Flume

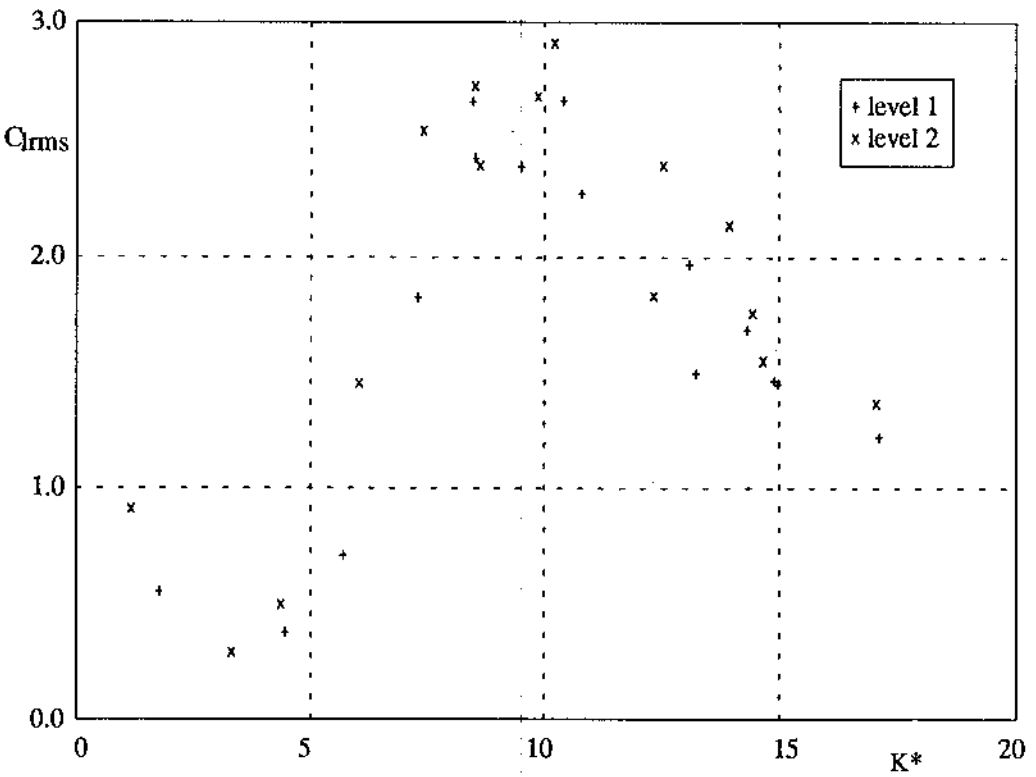

Figure 10 Cl(rms) v's K* - regular waves at the Delta Flume

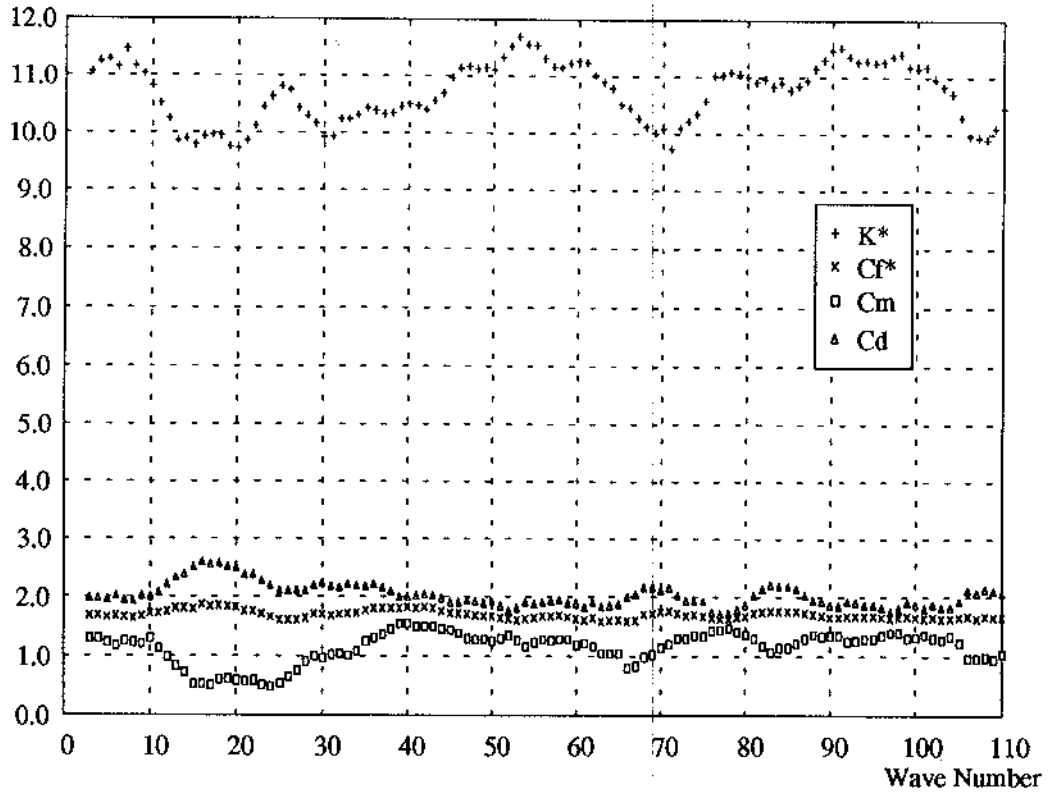

Figure 11 Variation of coefficients for regular wave run RC108

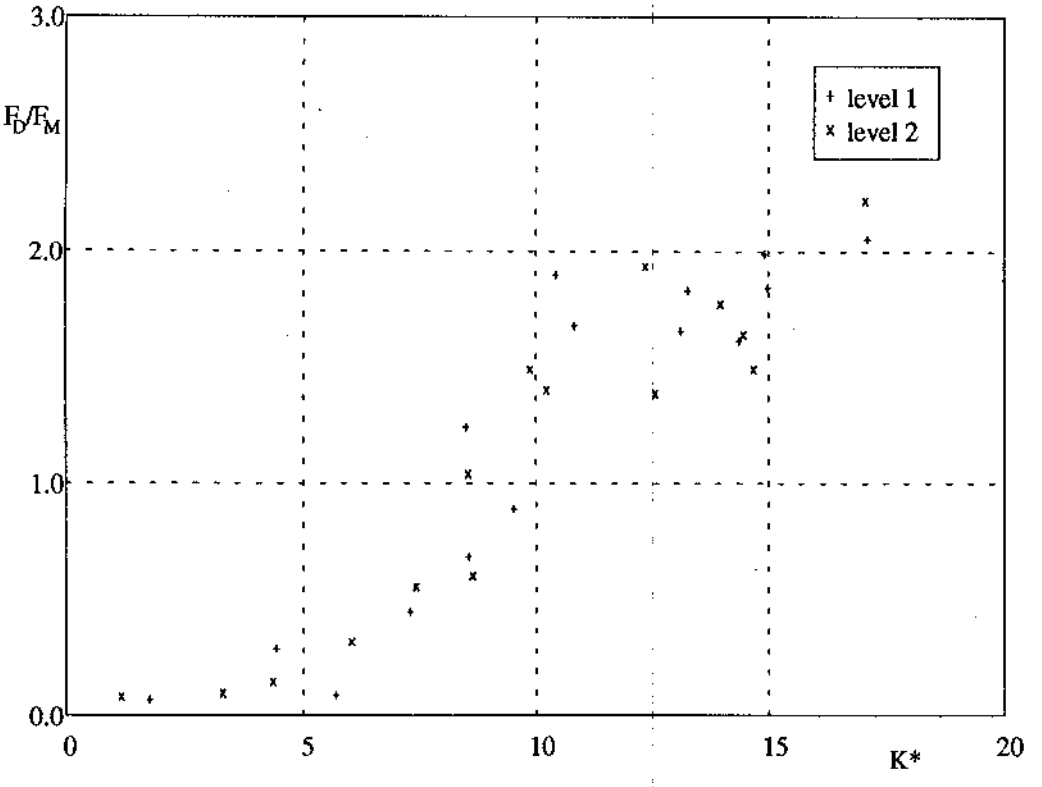

Figure 12 Ratio of rms drag force to rms inertia force for Delta Flume waves

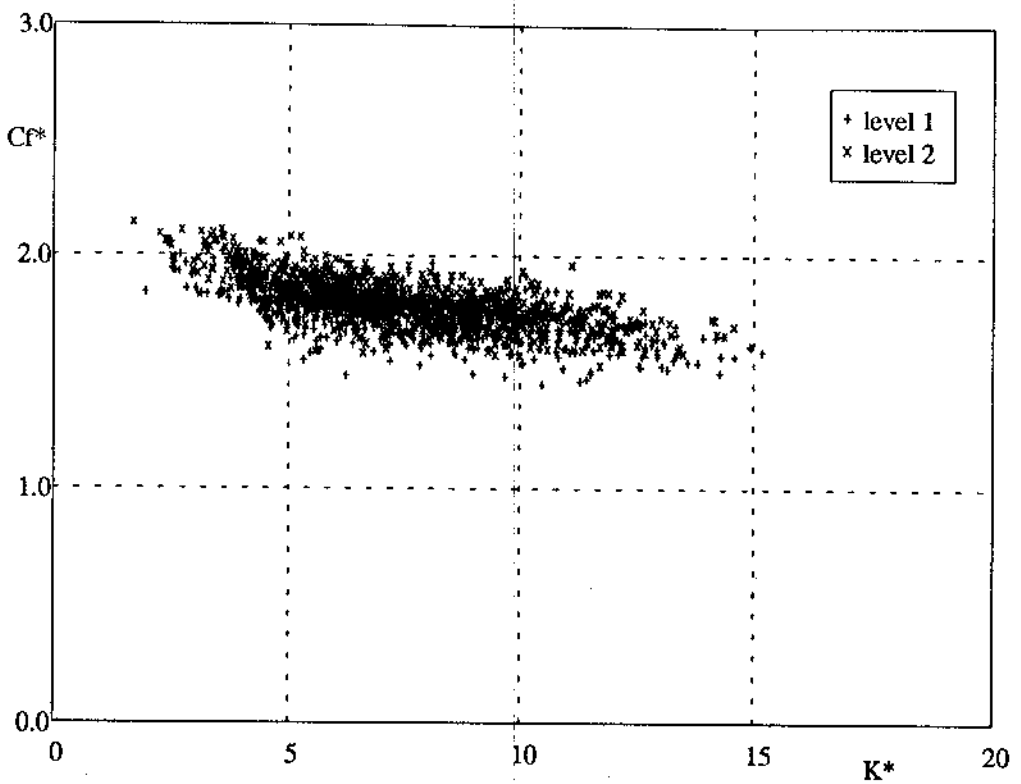

Figure 13 Cf* v's K* - random waves at the Delta Flume

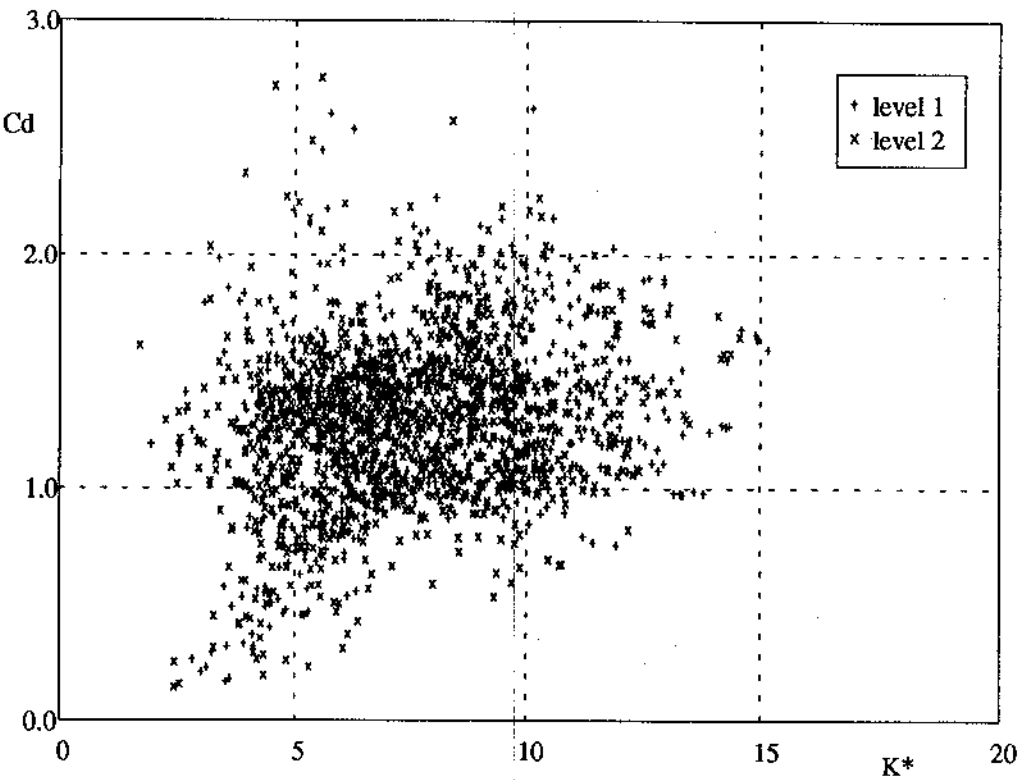

Figure 14 Cd v's K* - random waves at the Delta Flume

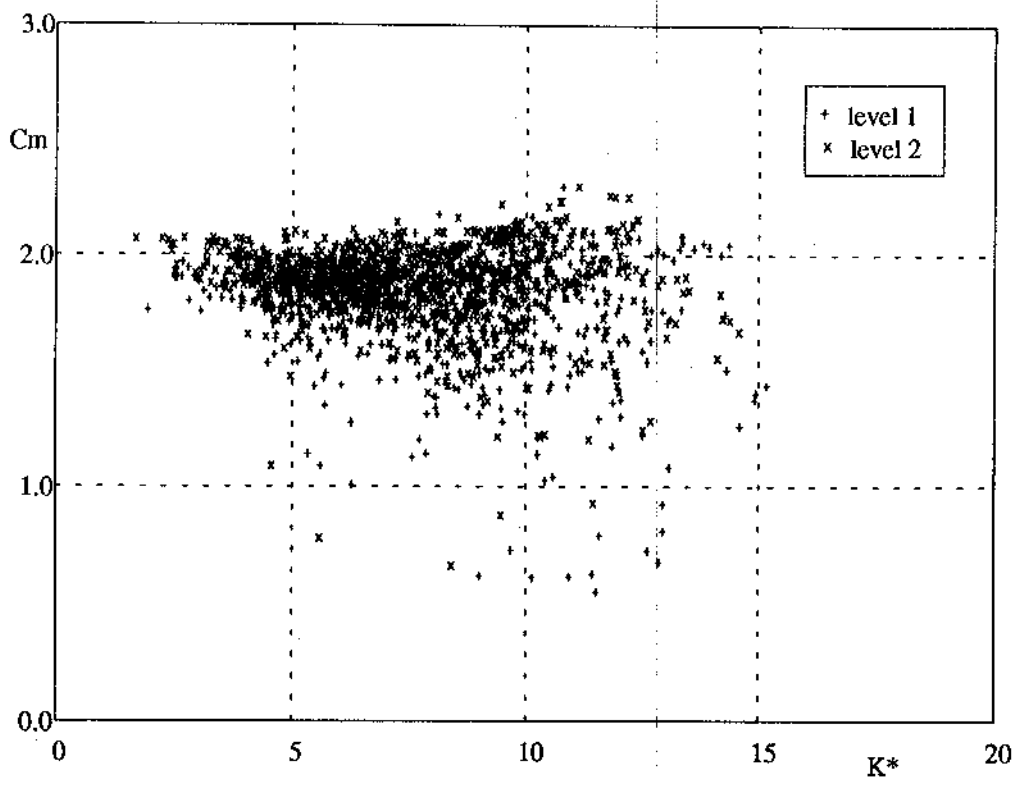

Figure 15 Cm v's K* - random waves at the Delta Flume

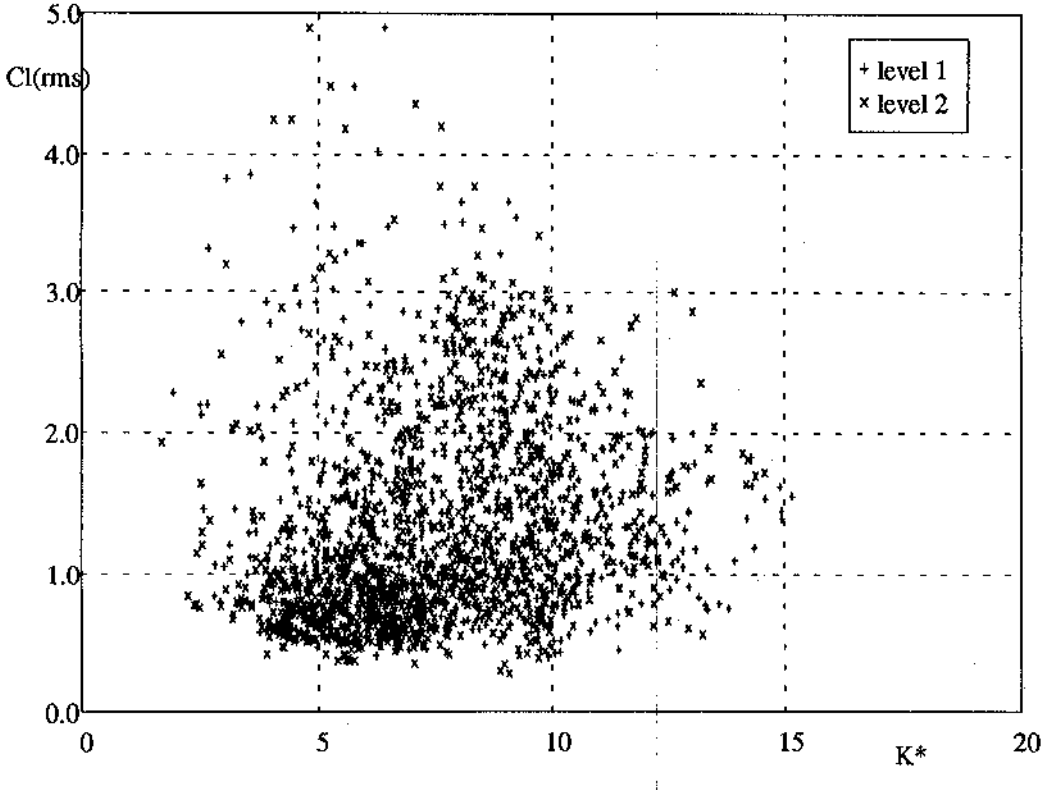

Figure 16 Cl(rms) v's K* - random waves at the Delta Flume

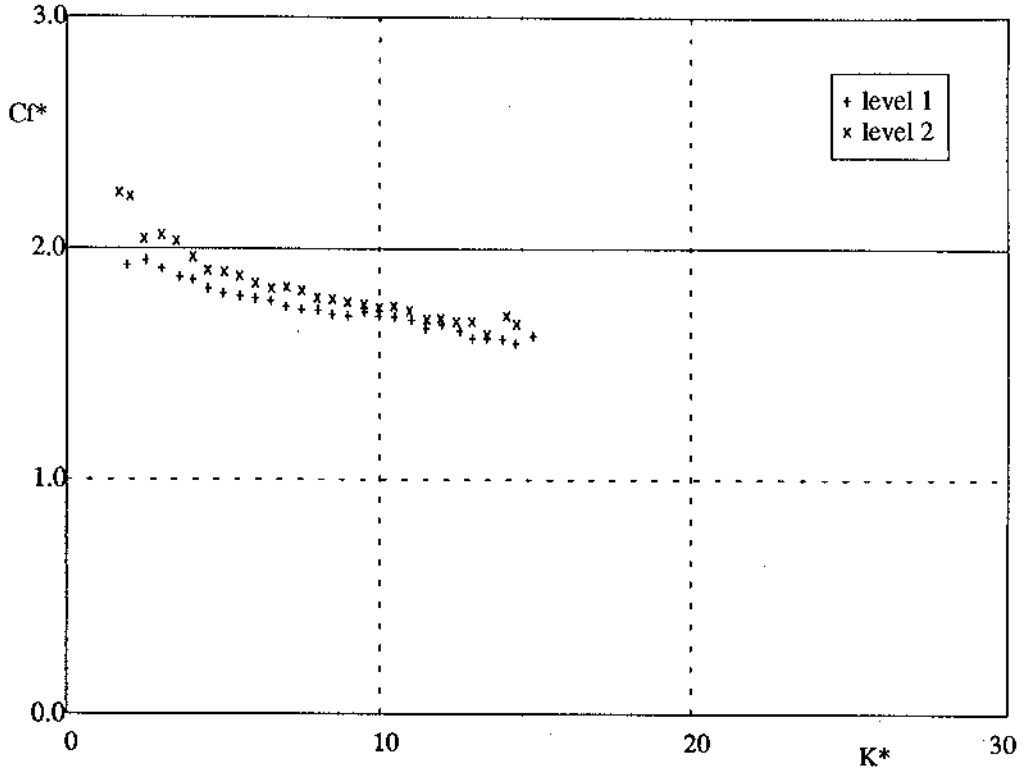

Figure 17 Mean values of Cf* v's K* for random waves at the Delta Flume

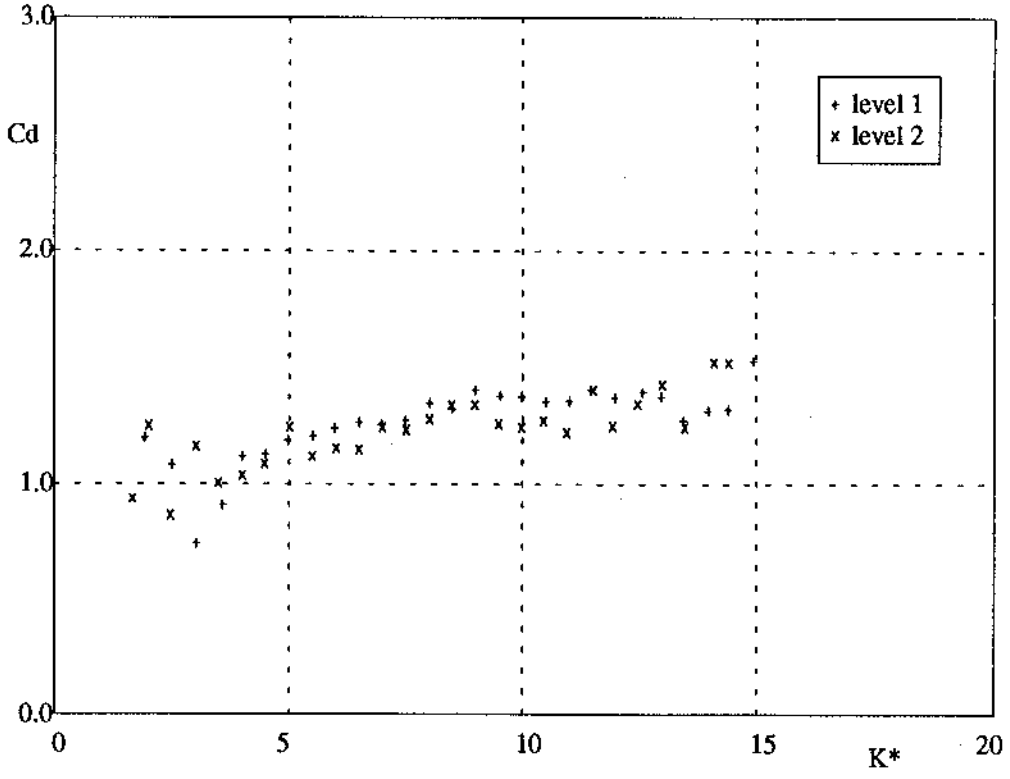

Figure 18 Mean values of Cd v's K* - random waves at the Delta Flume

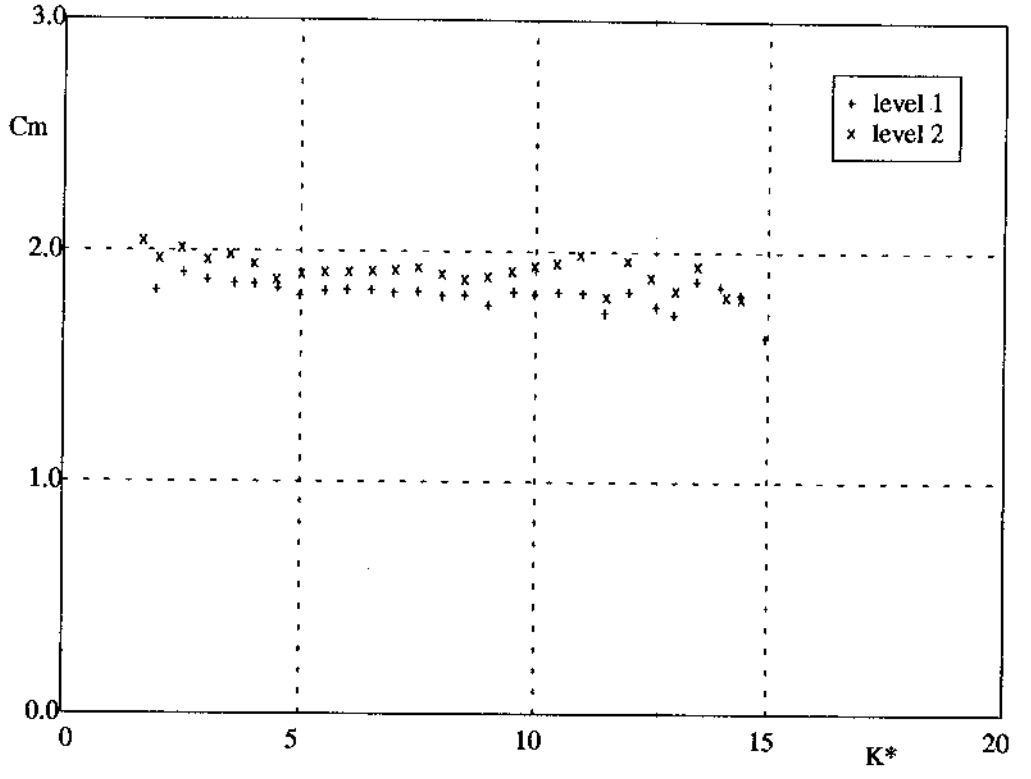

Figure 19 Mean values of Cm v's K* - random waves at the Delta Flume

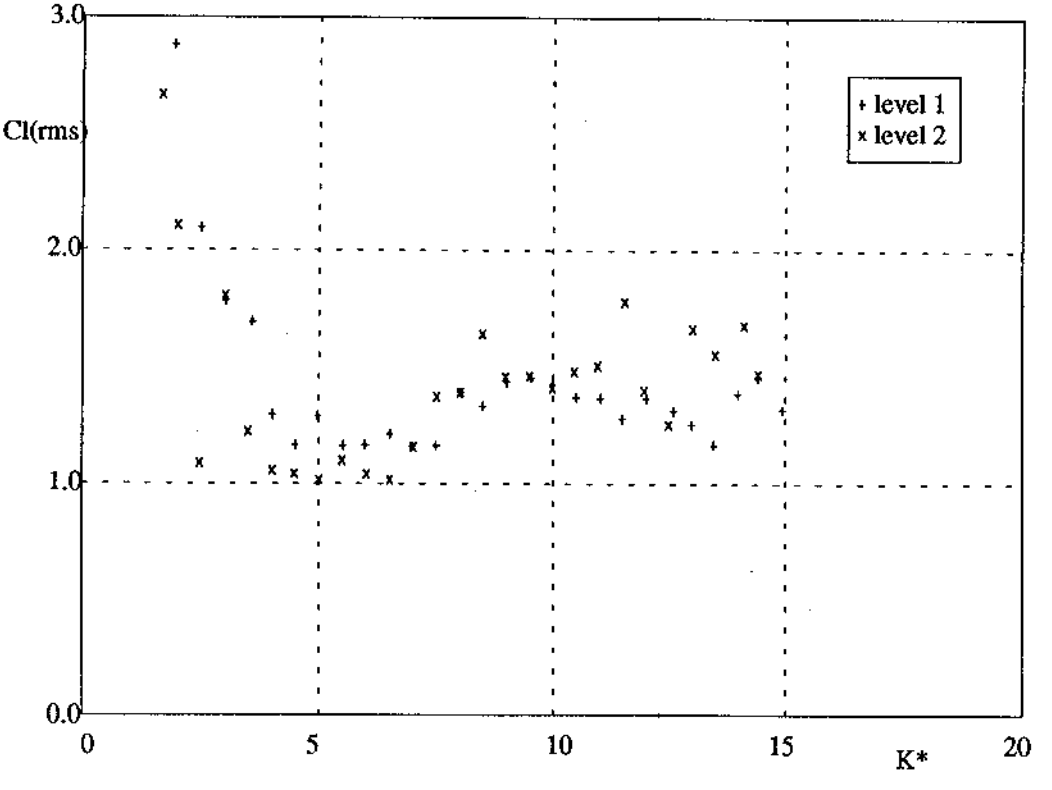

Figure 20 Mean values of Cl(rms) v's K* - random waves at the Delta Flume

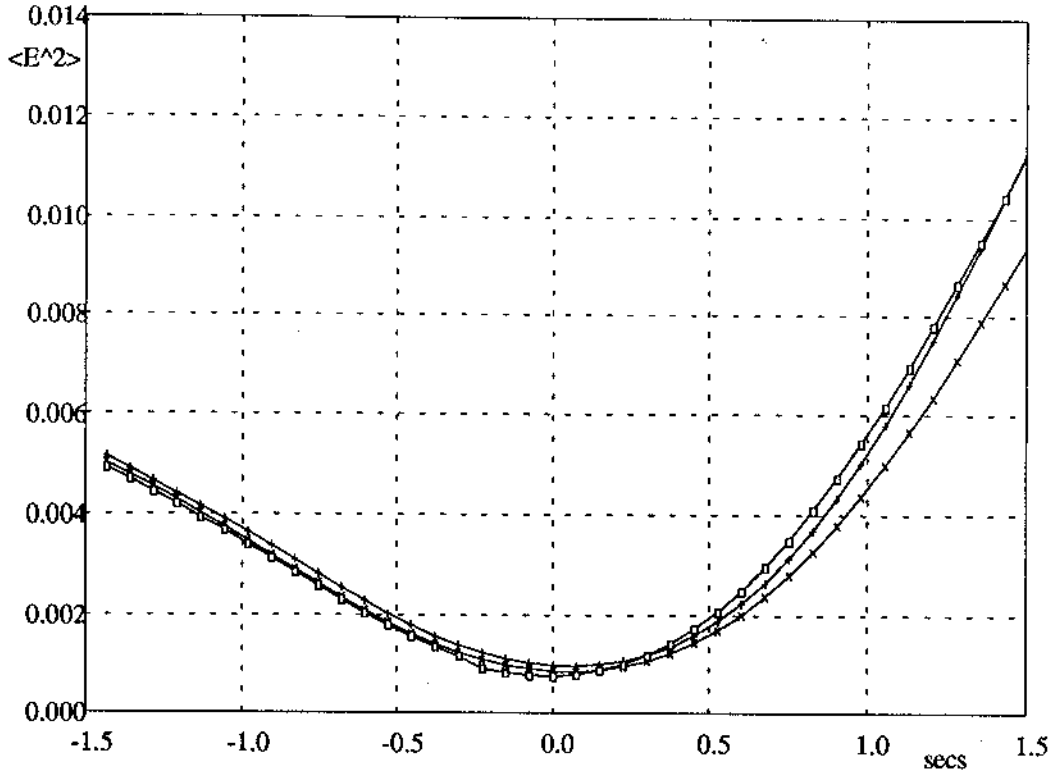

Figure 21 Typical error functions for CBT analysis

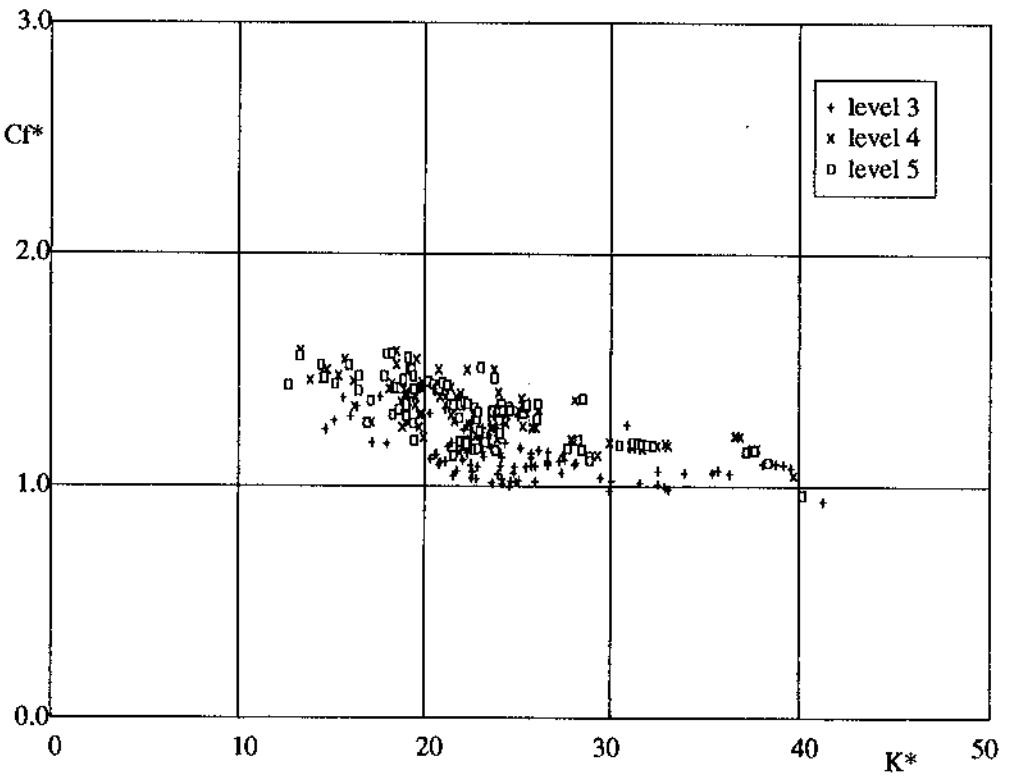

Figure 22 Cf* v's K* - CBT record 14

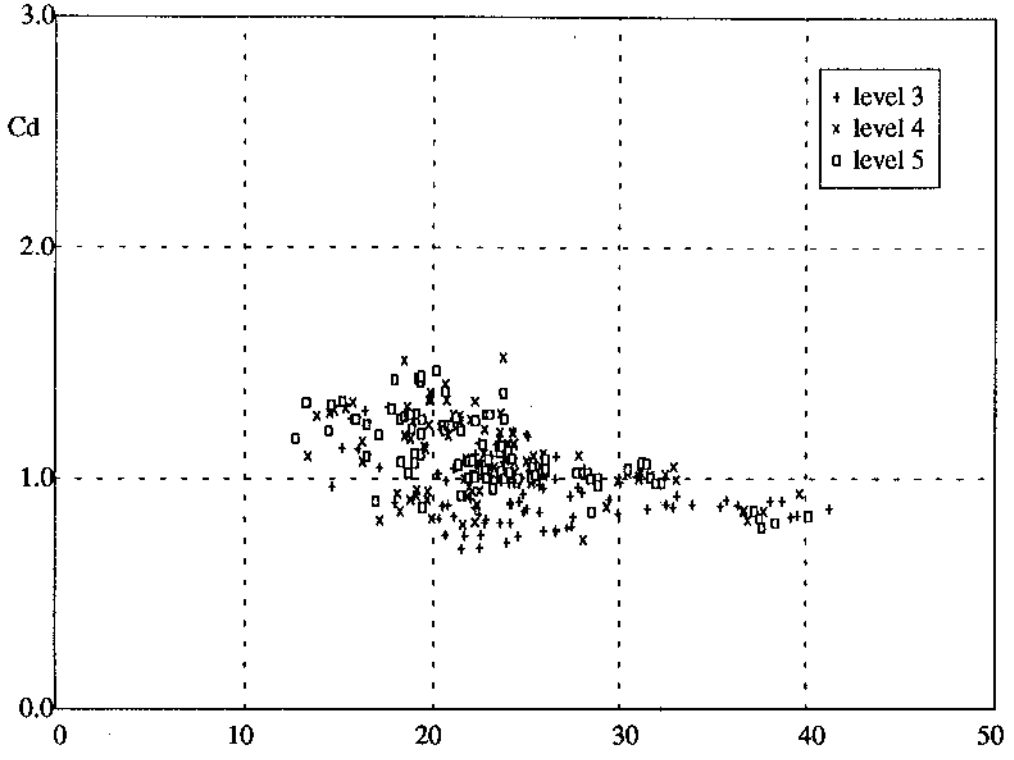

Figure 23 Cd v's K* - CBT record 14

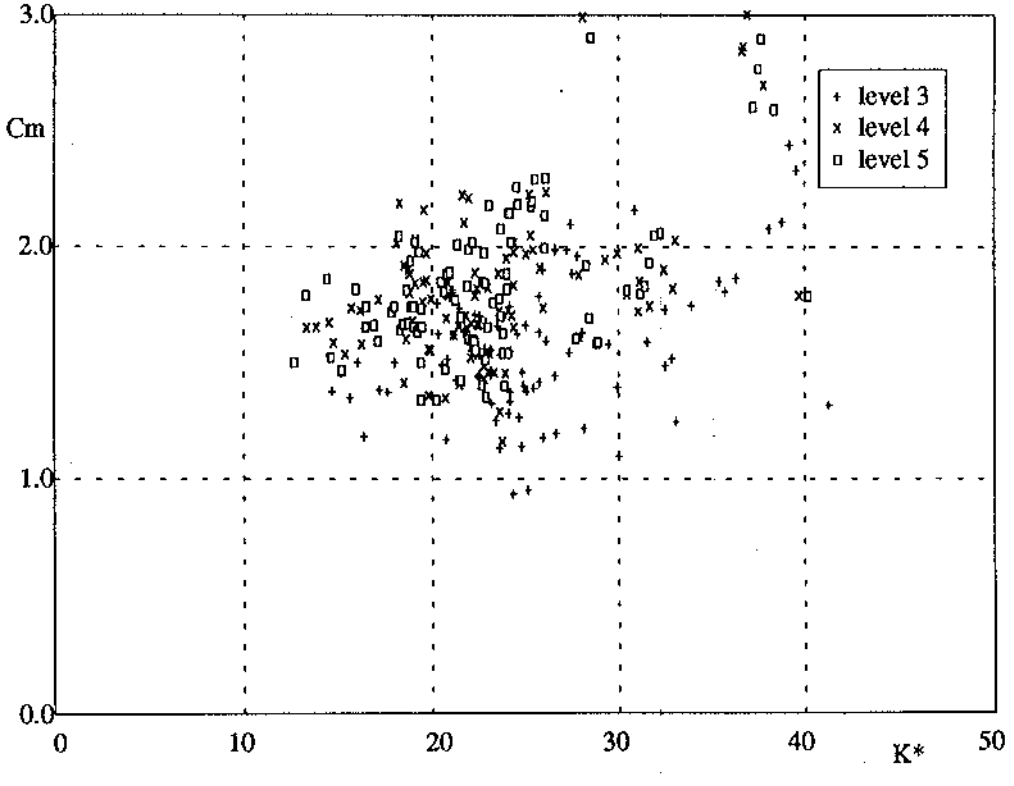

Figure 24 Cm v's K* - CBT record 14

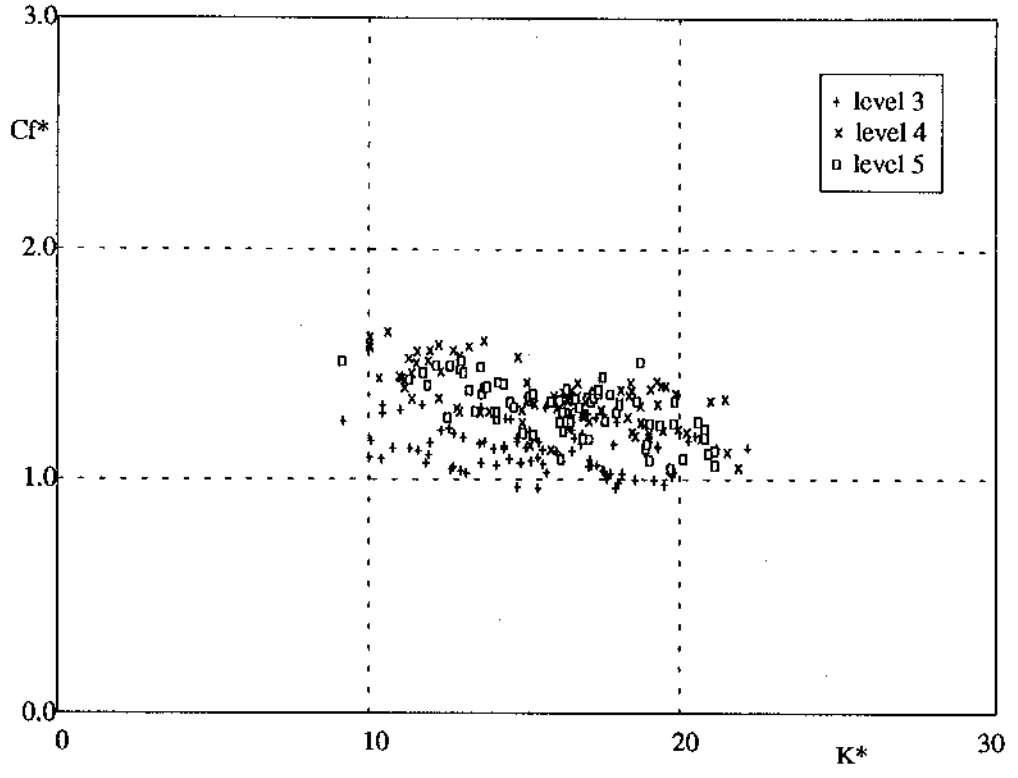

Figure 25 Cf* v's K* - CBT record 39

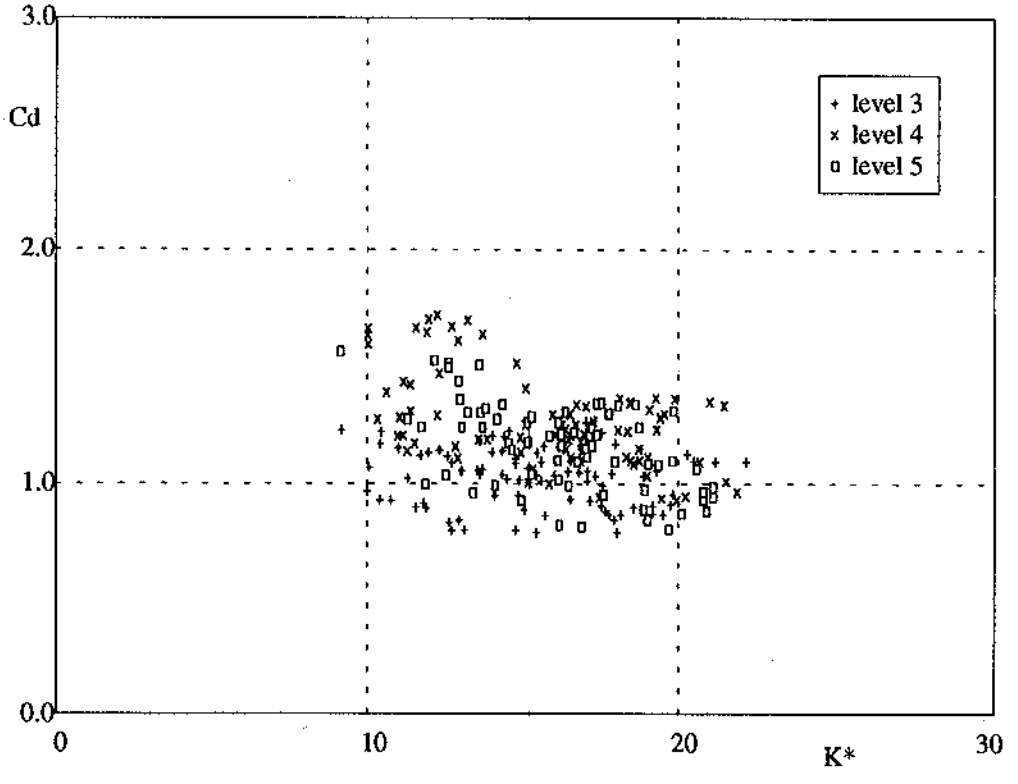

Figure 26 Cd v's K* - CBT record 39

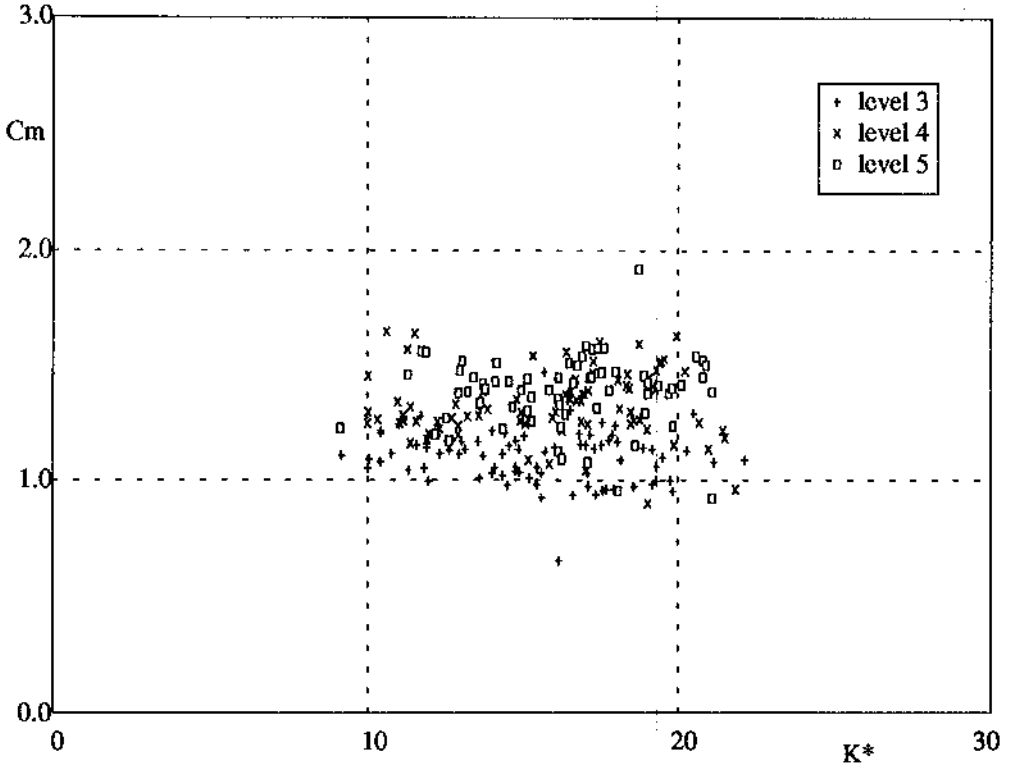

Figure 27 Cm v's K* - CBT record 39

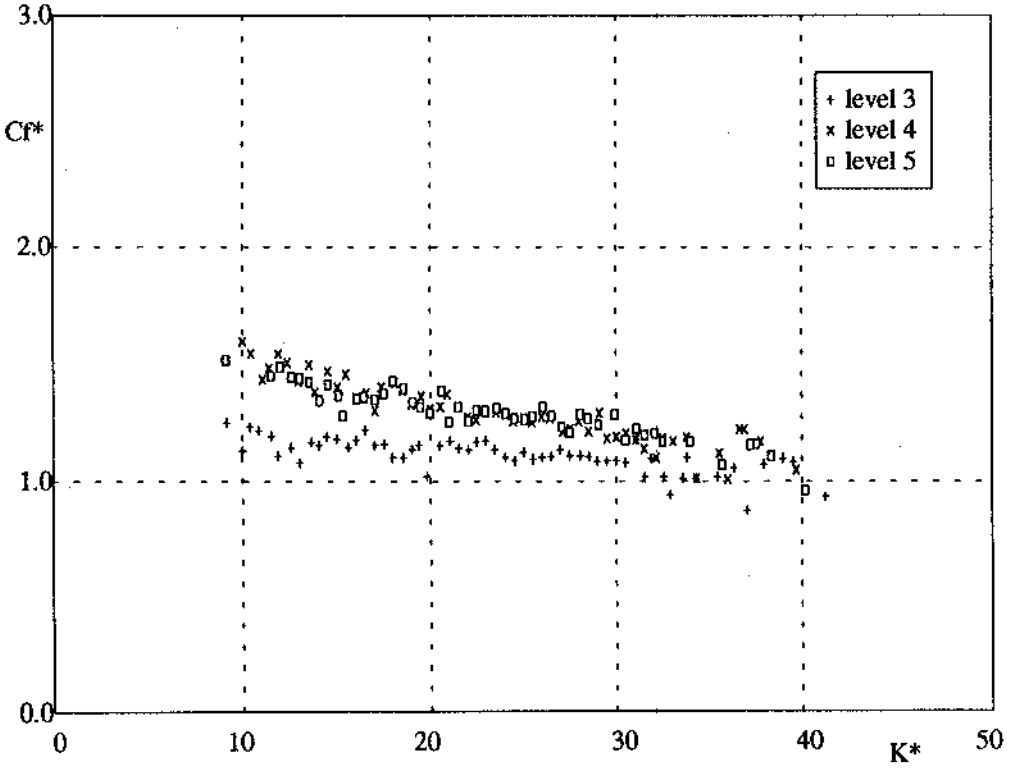

Figure 28 Mean values of Cf* v's K* - CBT records 14,15,19,28,39

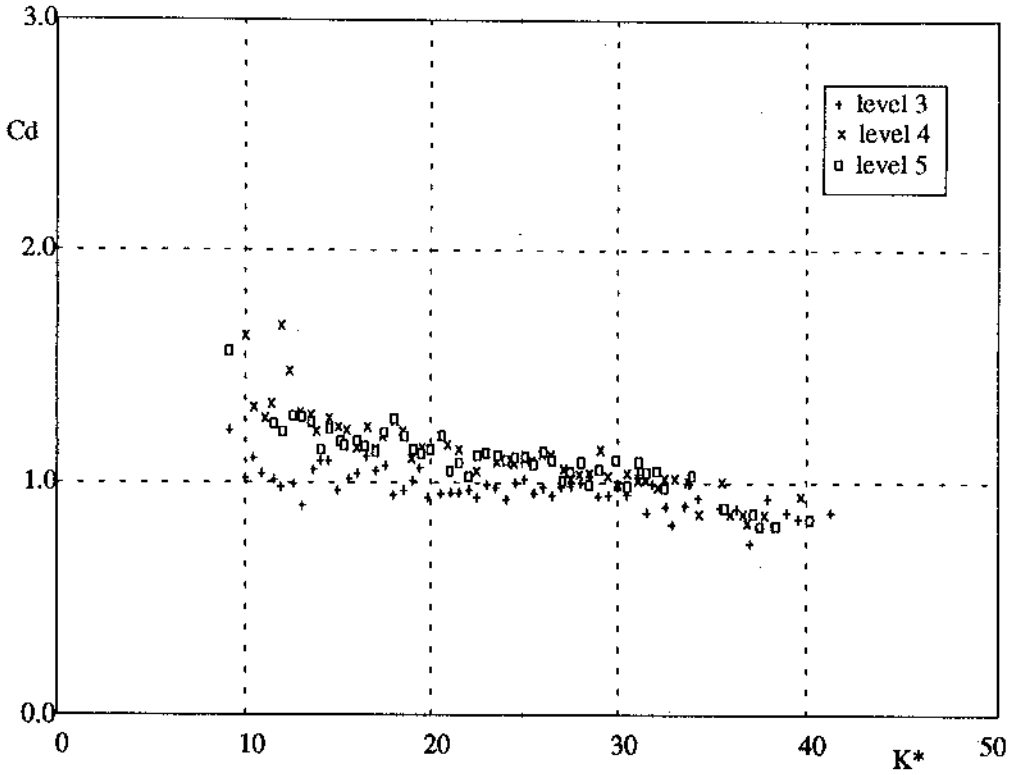

Figure 29 Mean values of Cd v's K* - CBT records 14,15,19,28,39

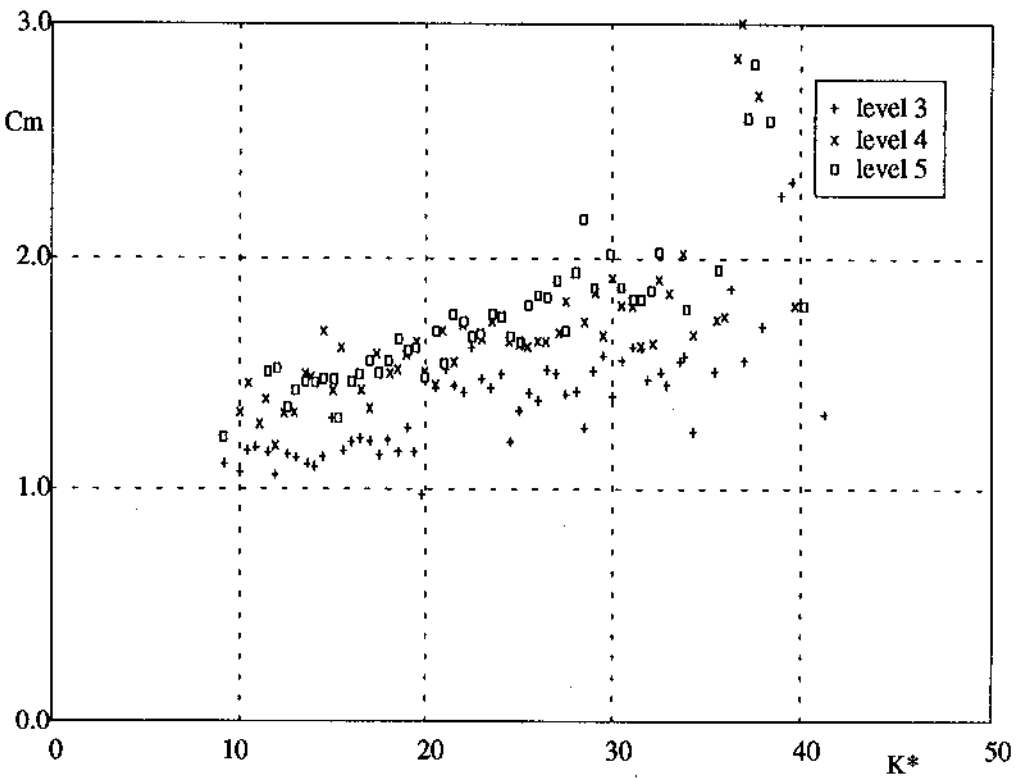

Figure 30 Mean values of Cm v's K* - CBT records 14,15,19,28,39

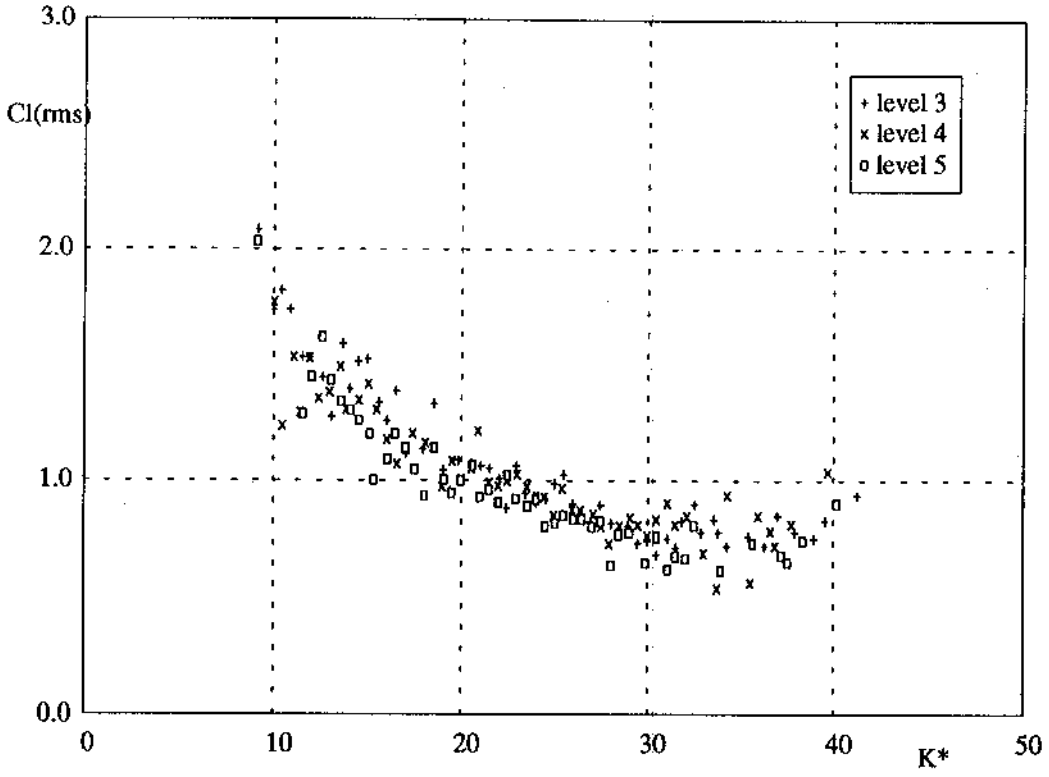

Figure 31 Mean values of Cl(rms) v's K* - CBT records 14,15,19,28,39

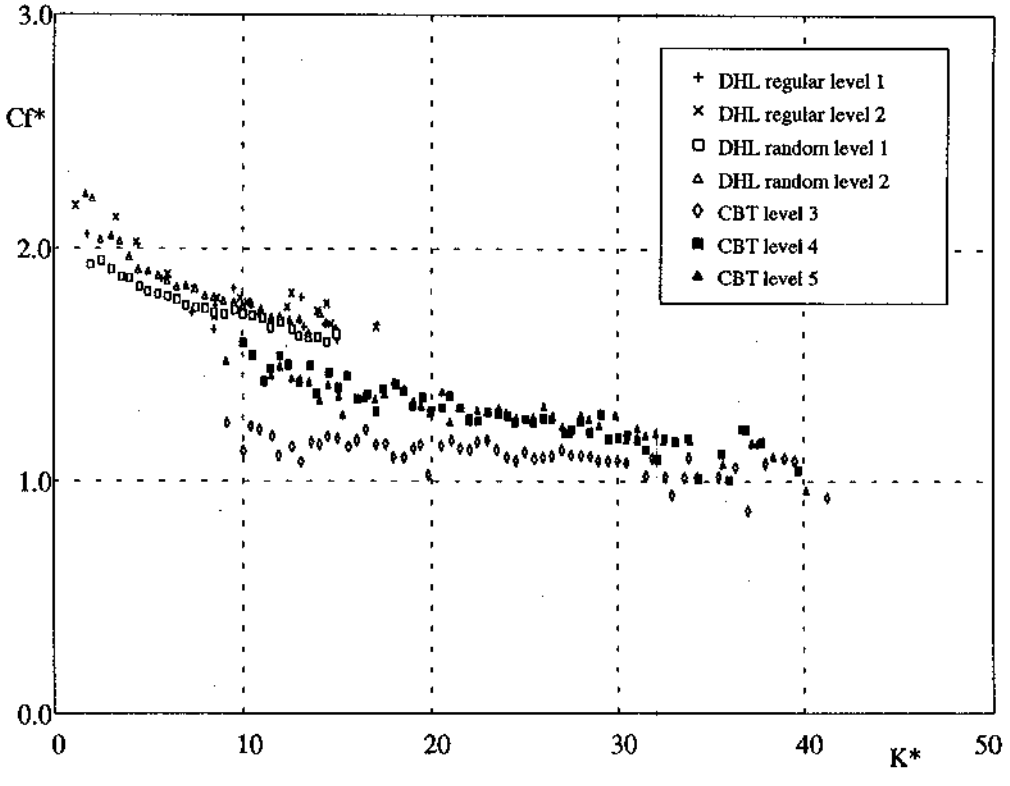

Figure 32 Cf* v's K* - all data

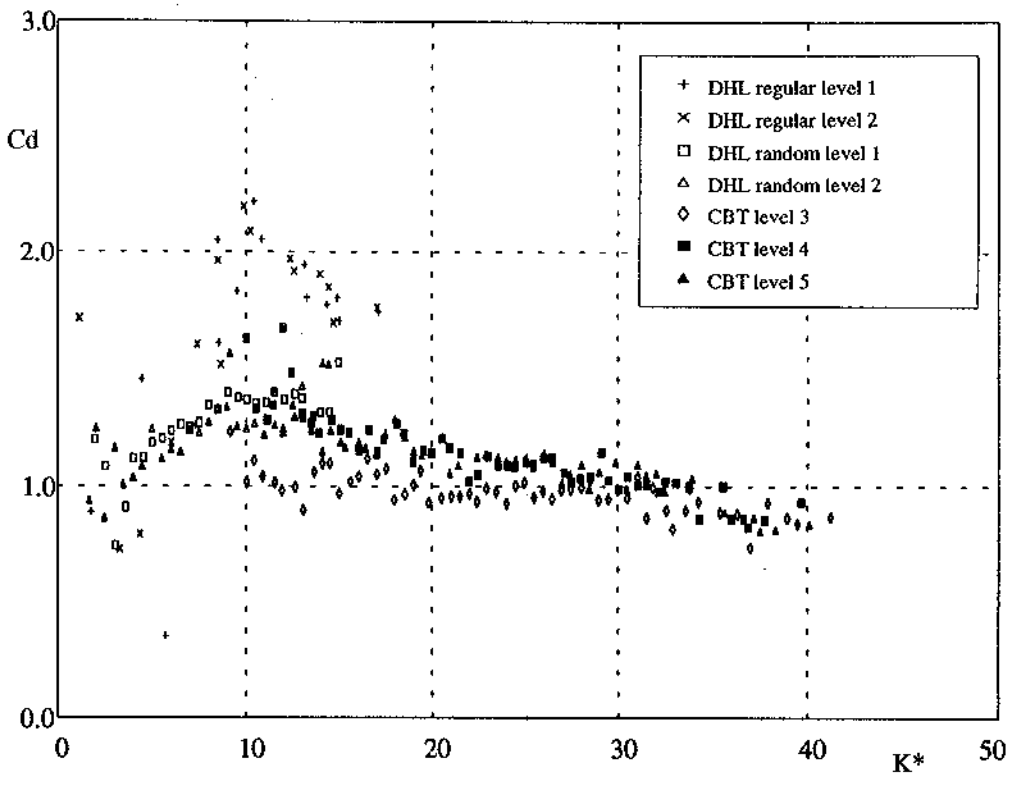

Figure 33 Cd v's K* - all data

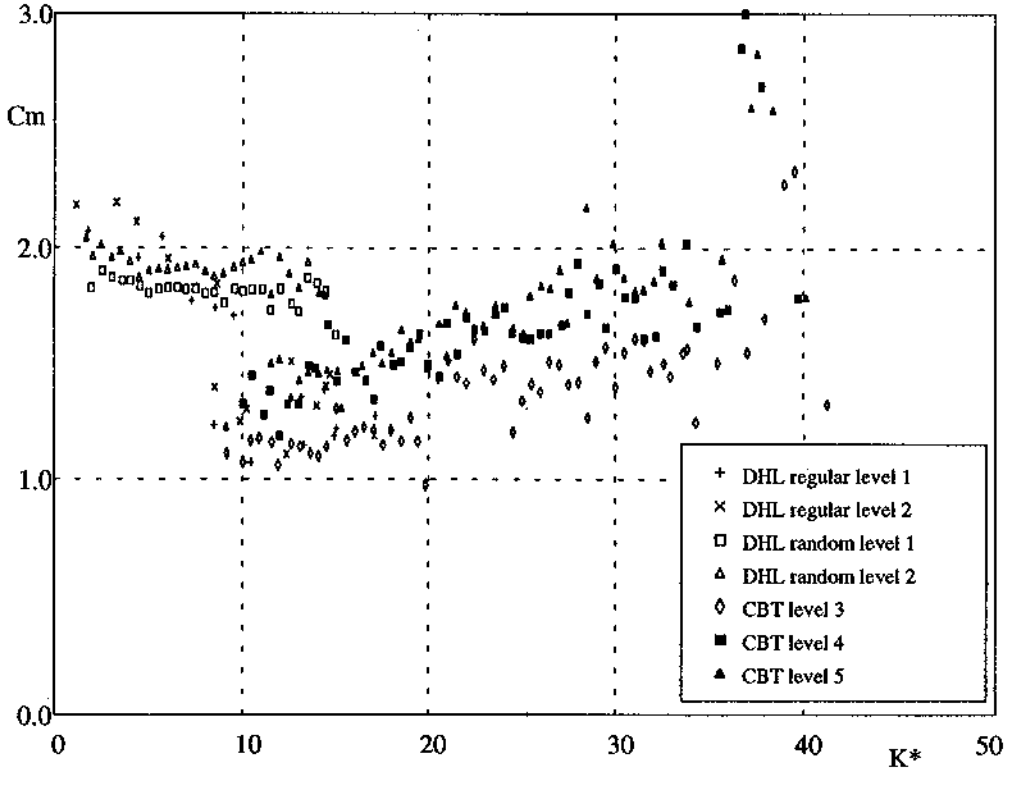

Figure 34 Cm v's K* - all data

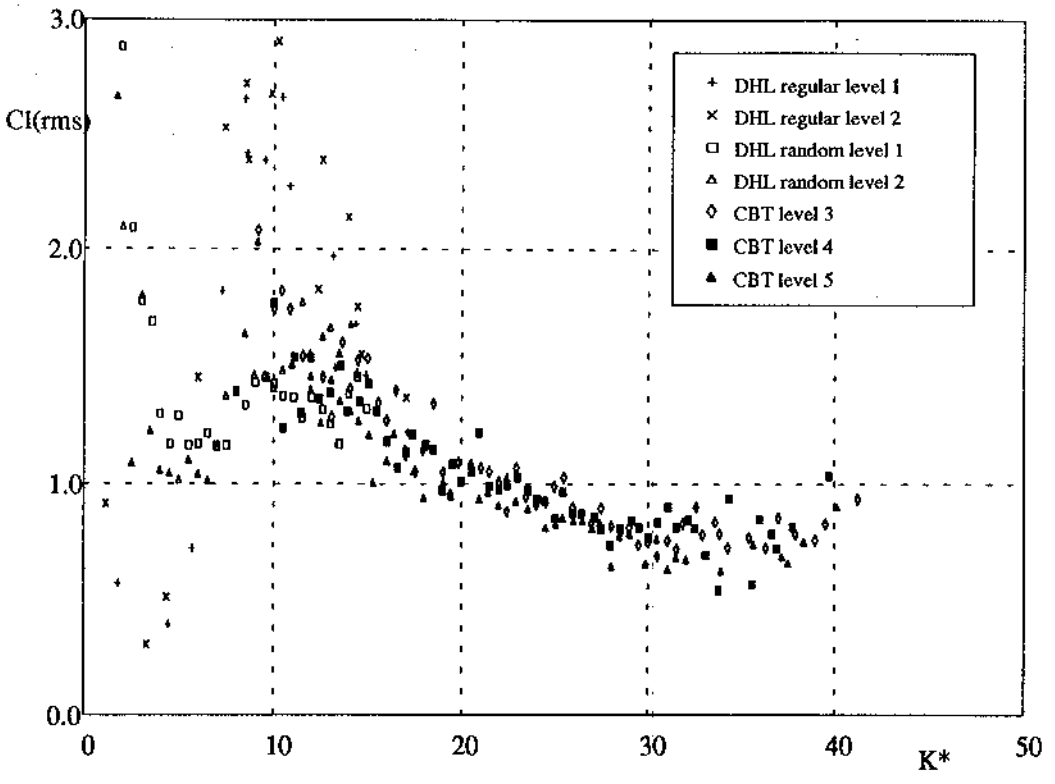

Figure 35 Cl(rms) v's K* - all data

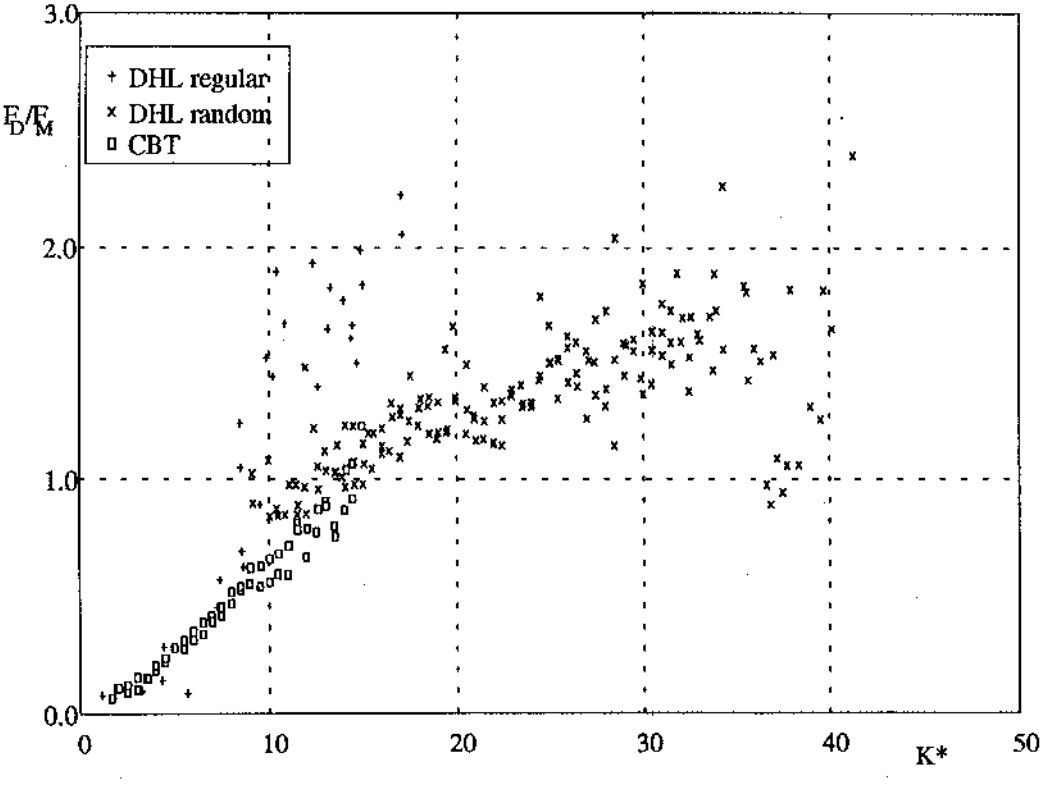

Figure 36 Ratio of rms drag force to rms inertia force - all data

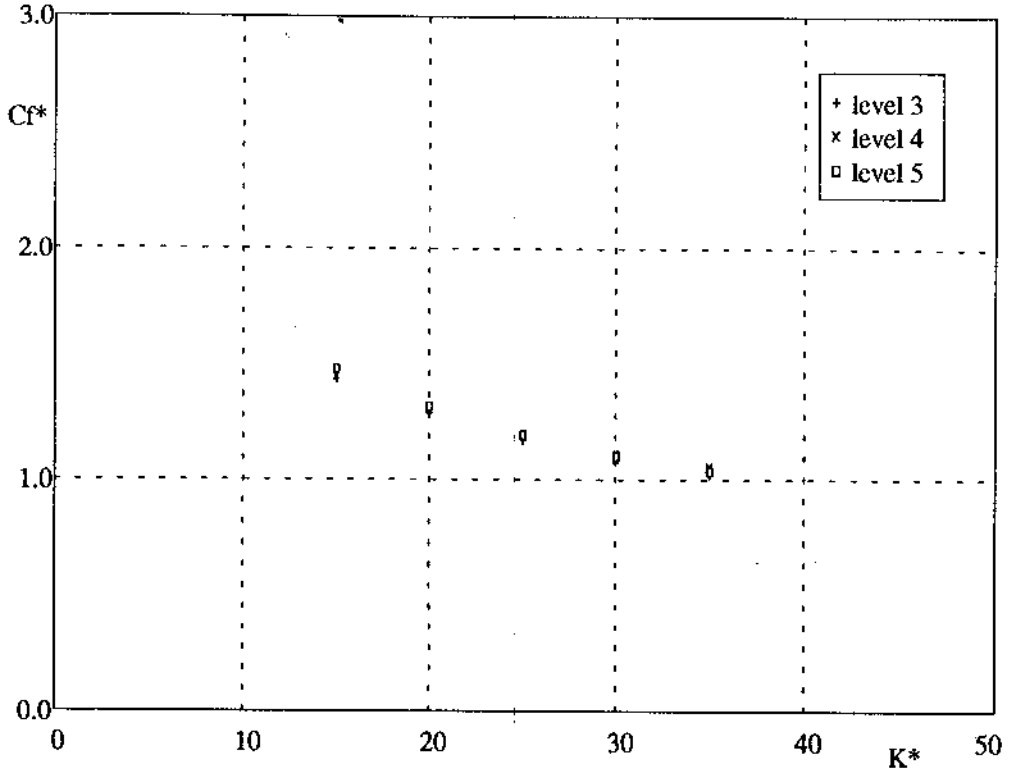

Figure 37 Cf* v's K* - CBT from Bishop[7]

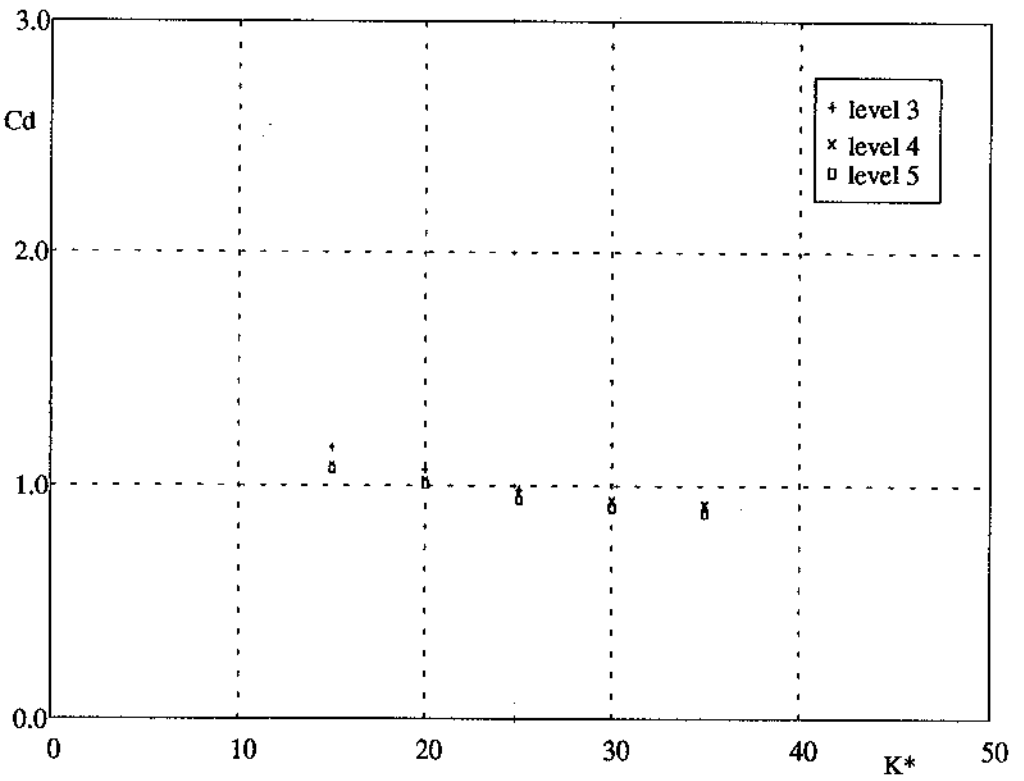

Figure 38 Cd v's K* - CBT from Bishop [7]

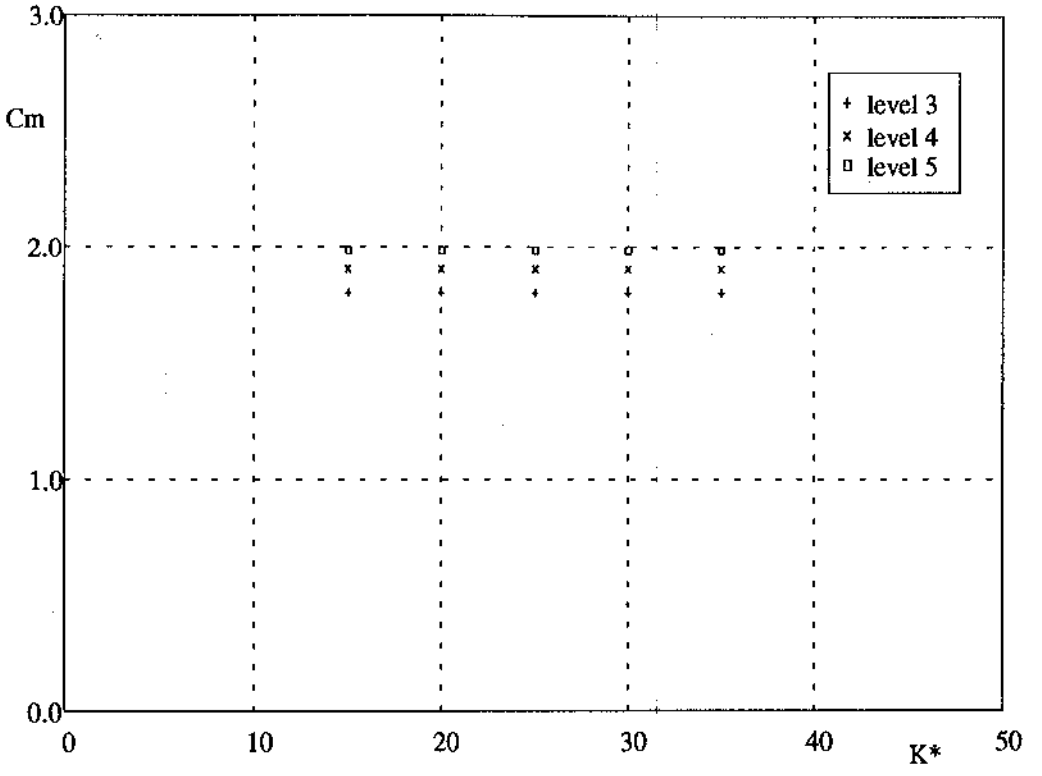

Figure 39 Cm v's K* - CBT from Bishop [7]

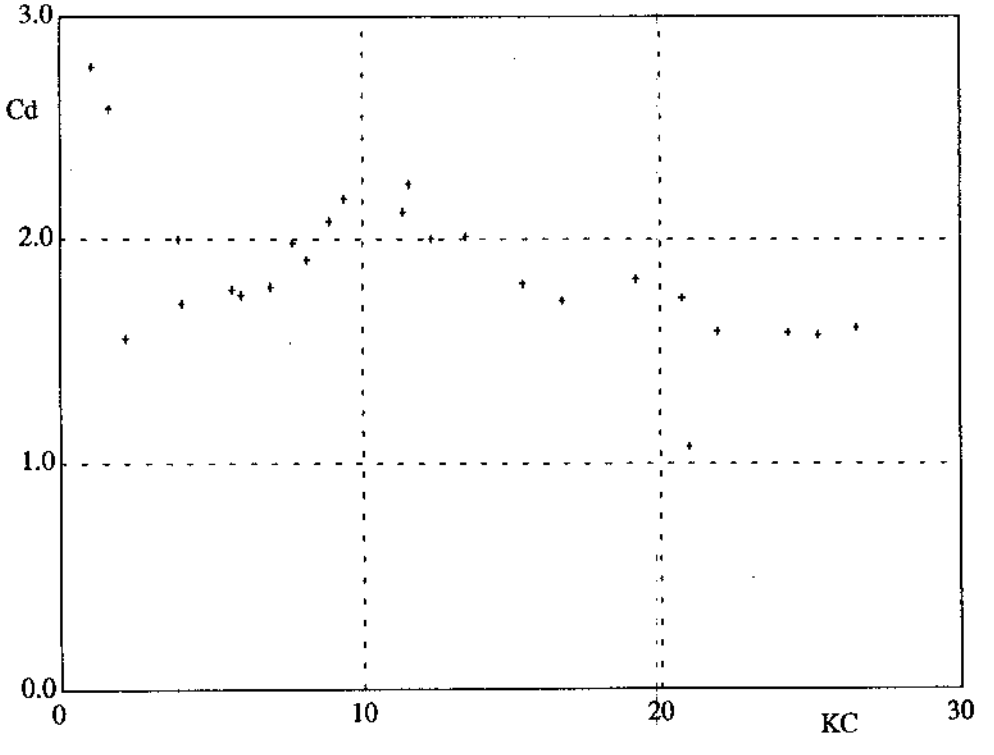

Figure 40 Cd v's KC - Delta Flume regular waves form Wolfram[10]

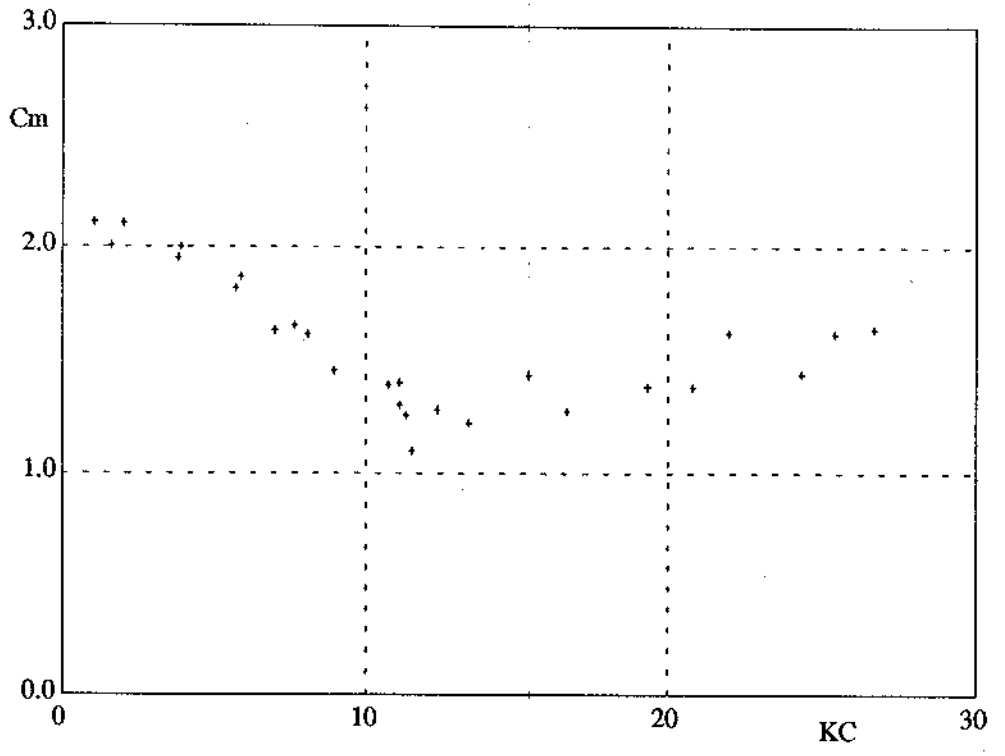

Figure 41 Cm v's KC - Delta Flume regular waves from Wolfram[10]

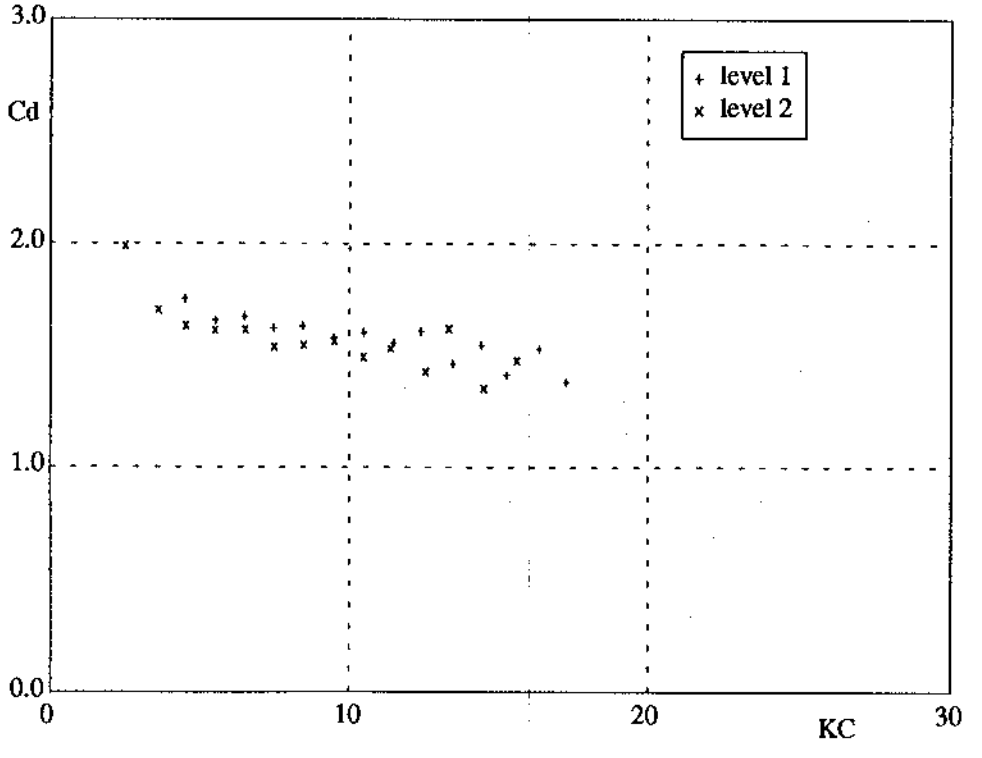

Figure 42 Cd v's KC - Delta Flume random waves from Davies[8]

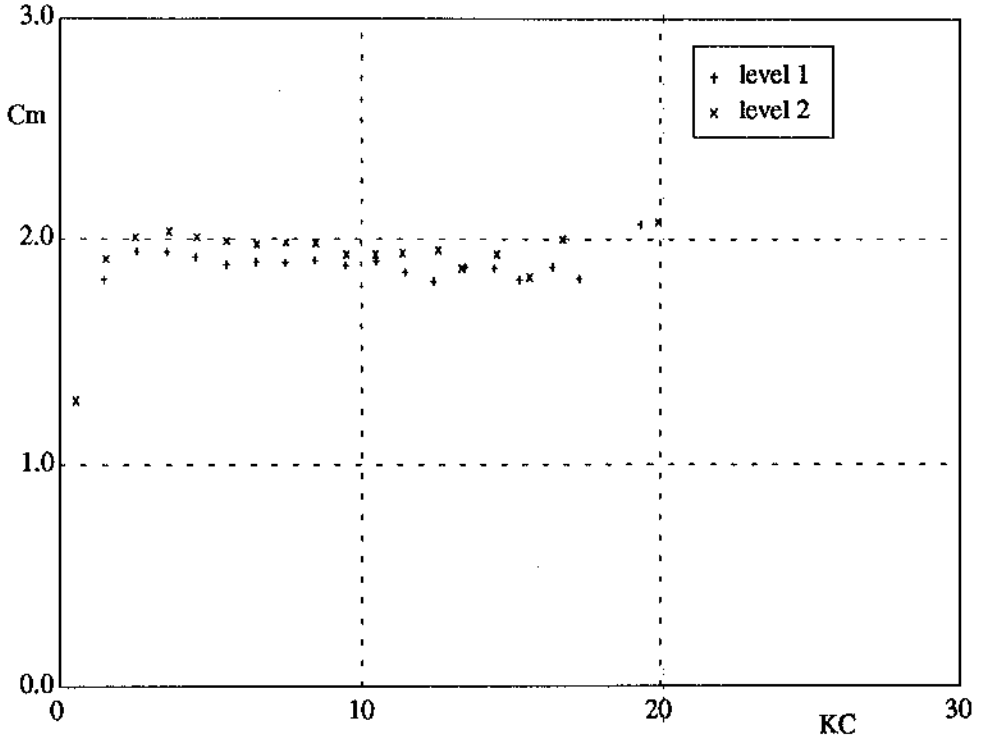

Figure 43 Cm v's KC - Delta Flume random waves from Davies[8]

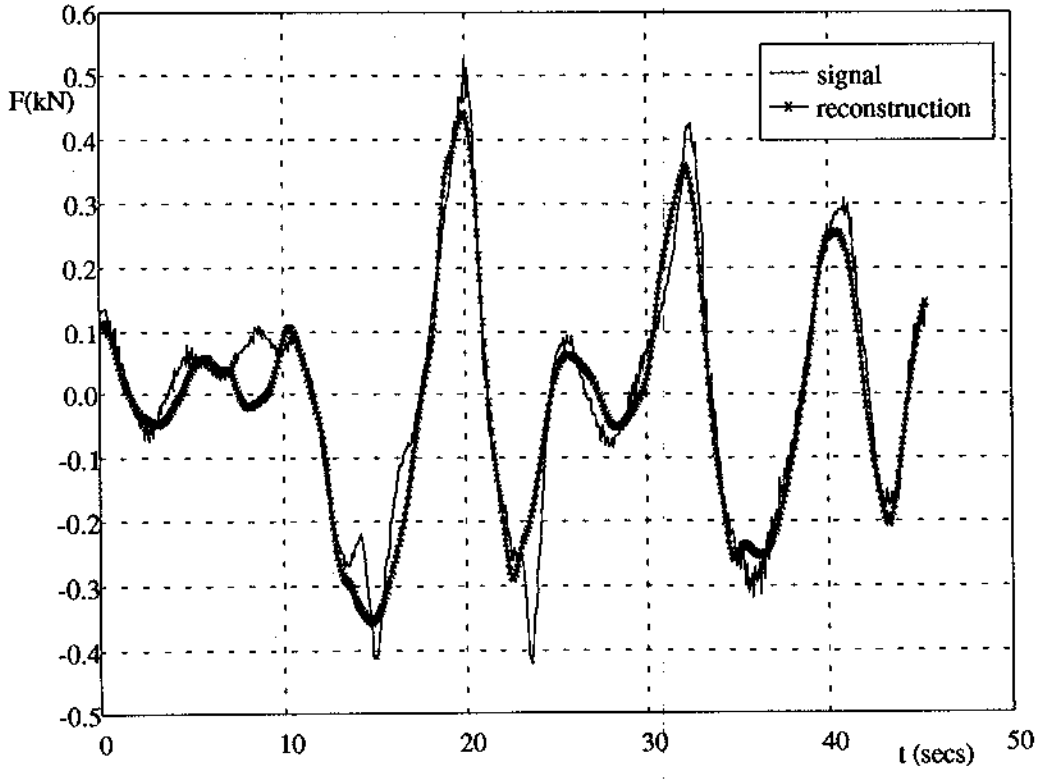

Figure 44 Morison force reconstruction for CBT data K* = 20.85

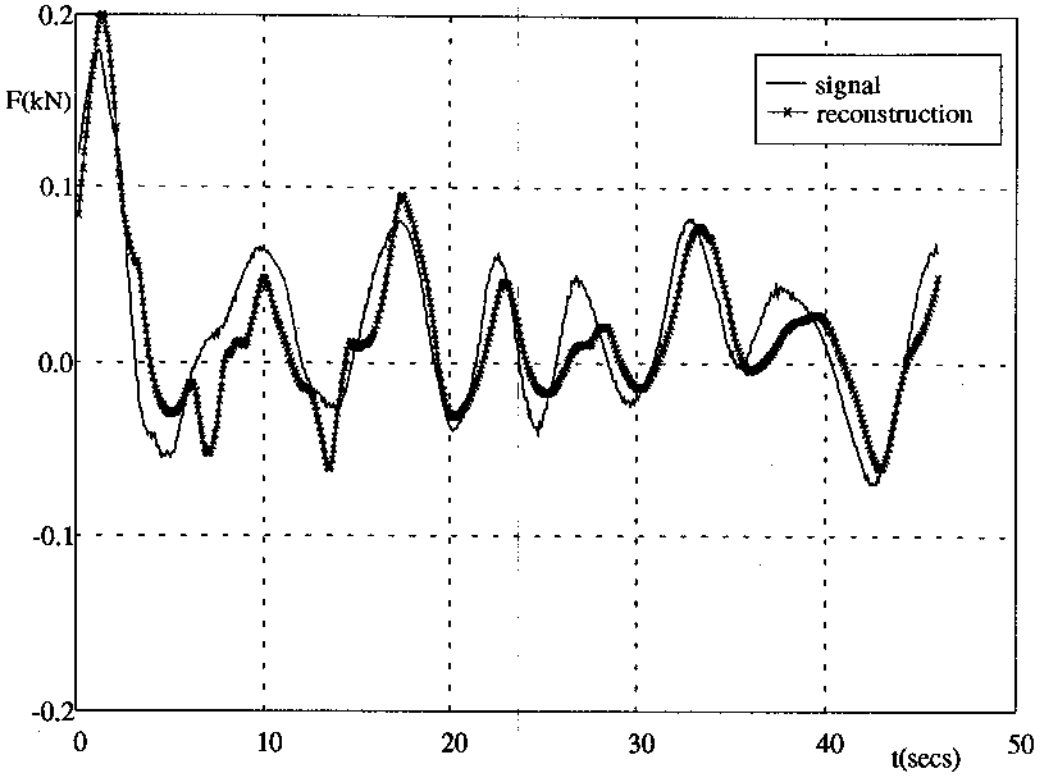

Figure 45 Morison force reconstruction K* = 12.97

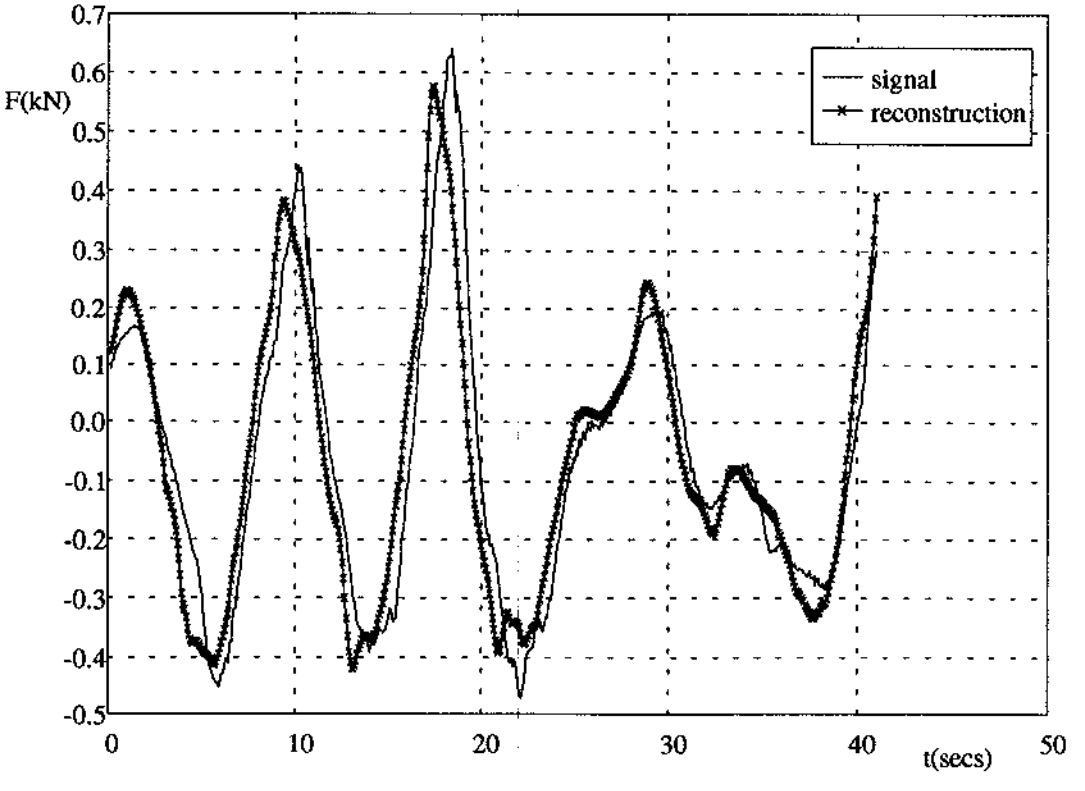

Figure 46 Morison force reconstruction K* = 27.92

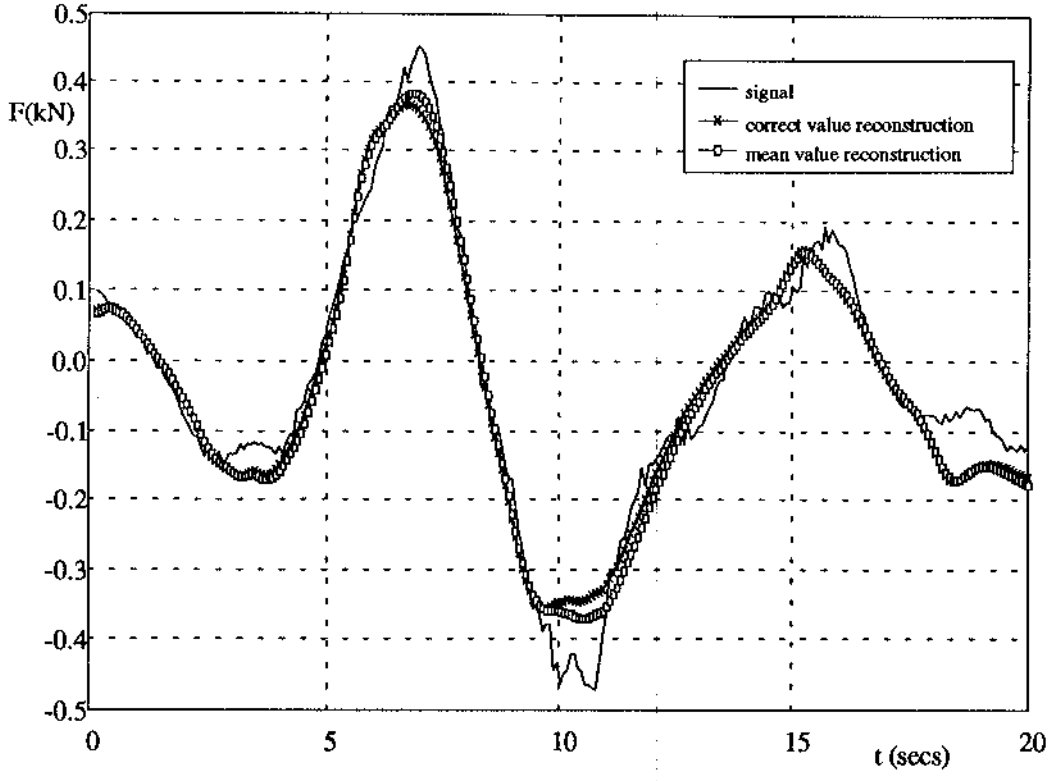

Figure 47 Morison force reconstruction using different coefficients, K* = 20.55

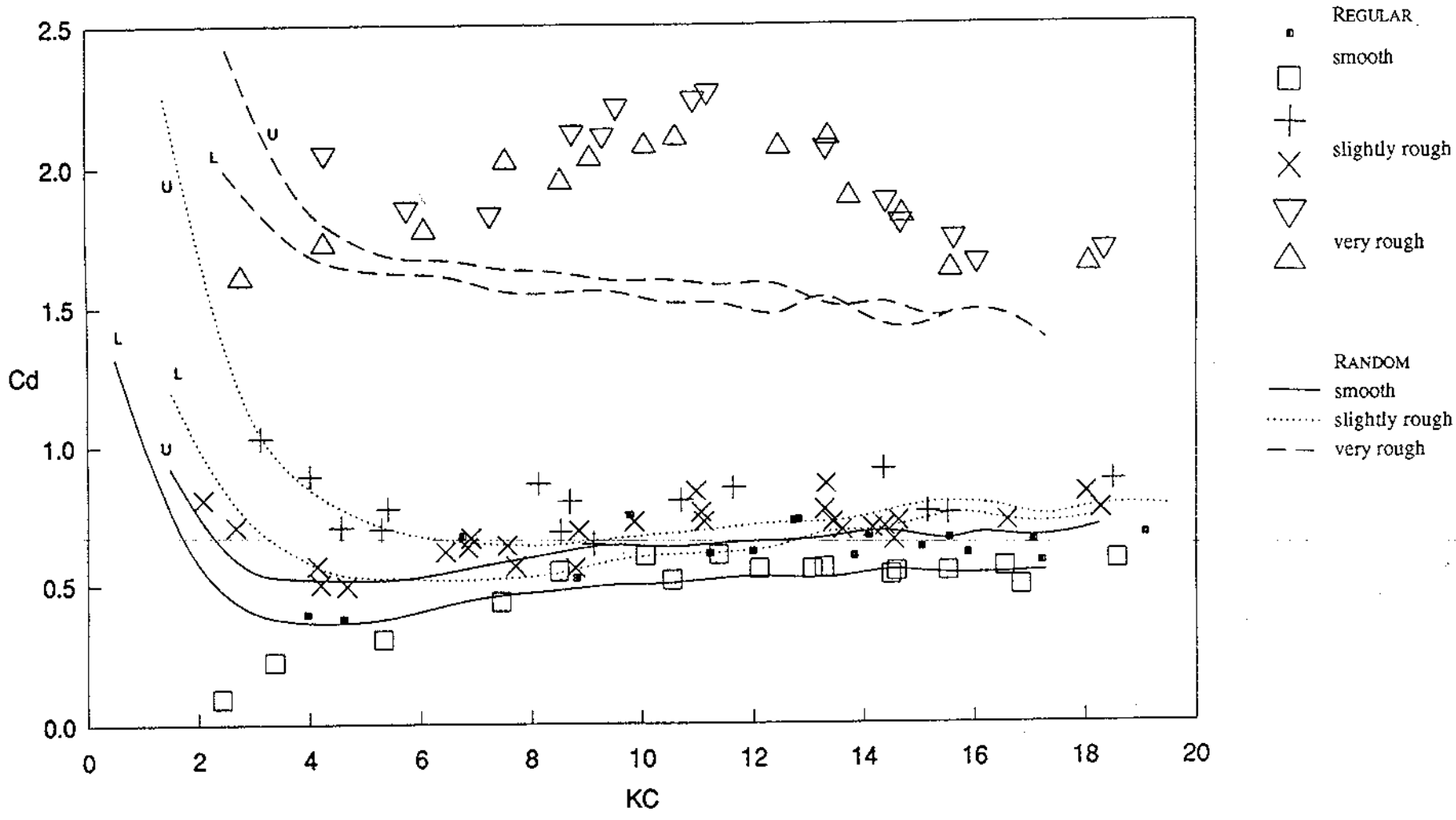

Figure 48 Cd v's KC for smooth and rough cylinders in random waves at DHL (reproduced from Davies [8], figure 6.6)

HSE
BOOKS

MAIL ORDER
HSE priced and free
publications are
available from:
HSE Books
PO Box 1999
Sudbury
Suffolk CO10 6FS
Tel: 01787 881165
Fax: 01787 313995

RETAIL
HSE priced publications
are available from
good booksellers.

HEALTH AND SAFETY ENQUIRIES
HSE InfoLine
Tel: 0541 545500
or write to:
HSE Information Centre
Broad Lane
Sheffield S3 7HQ

ISBN 0-7176-0999-5

£15.00 net